COSMO

A Prospectus for the Design, Construction, and Operation of a

COronal Solar Magnetism Observatory

The National Center for Atmospheric Research
High Altitude Observatory
Steven Tomczyk, Principal Investigator

The University of Hawaii
Haosheng Lin, Co-Principal Investigator

The University of Michigan
Thomas Zurbuchen, Co-Principal Investigator

31 January, 2008

1 EXECUTIVE SUMMARY

Measuring magnetic fields in the solar corona is crucial to understanding and predicting the Sun's generation of space weather that affects communications, space flight, and power transmission. Most solar activity, including high-energy electromagnetic radiation, solar energetic particles, flares, and coronal mass ejections, derive their energy from coronal magnetic fields. The corona is also the source of the solar wind with its embedded magnetic field that engulfs the Earth. Because changes in solar magnetic fields drive space weather, the ability to measure these changes will help us understand the underlying physical processes and could lead to improved predictions of hazardous effects on Earth.

Coronal magnetic field measurements at the required sensitivity and cadence are not possible with current instruments. These measurements are difficult because the corona is nearly one million times less bright than the solar disk, but much higher in temperature. These conditions make the emission lines used to measure coronal magnetic fields extremely weak and broad. Thus, a large-aperture telescope is needed to accurately measure these faint signals.

New prototype instrumentation developed at the University of Hawaii and at the NCAR High Altitude Observatory has demonstrated that measurements of coronal magnetic fields are now possible, using advanced infrared detector technology to observe weak forbidden lines. New scientific discoveries have already resulted from these breakthroughs, but current telescopes are too small to collect sufficient light at the necessary resolution and cadence. A ground-based facility that includes a large-aperture solar telescope and proven supporting instrumentation is a compelling next step to advance research into the solar corona.

We propose to build a COronal Solar Magnetism Observatory (COSMO) facility on a mountaintop in the Hawaiian Islands. The facility will take continuous synoptic measurements of the entire corona during the day in order to understand solar eruptive events that drive space weather and to investigate long-term and solar-cycle phenomena. The primary instrument will consist of a 1.5-m coronagraph with two detector systems: a narrow-band filter polarimeter and a spectropolarimeter. Supporting instruments are a white-light coronagraph to record the evolution of the electron scattered corona (K-corona) and a chromosphere and prominence magnetometer.

COSMO's unique observations of the global coronal magnetic field and its environment will enhance the value of data collected by other observatories on the ground (SOLIS, ATST, and FASR) and in space (SOHO, TRACE, GOES, Hinode, STEREO and SDO). COSMO observations will help meet primary goals of the National Space Weather Program (NSWP), the Solar Heliospheric and Interplanetary Environment (SHINE) program, and the NASA Living With a Star initiative. A better understanding of the solar atmosphere was called for by the National Research Council decadal review of research strategy in solar and space physics (Lanzerotti 2003), and the coronal magnetic field was identified as one of the top scientific priorities.

In addition to the unique measurement capabilities of the COSMO facility, maximum impact of the data collected will be assured by a program design that emphasizes scientific community involvement, especially with universities. A Science Advisory Panel, including experts from the solar, heliospheric, and space-weather communities, has developed targeted requirements for the COSMO facility. In the operational phase, the Science Advisory Panel will become a User Advisory Panel to govern facility allocations, identify data products, recommend instrument upgrades, and administer special observing campaigns. COSMO will have an open data policy, providing all observational data to the scientific community. The facility will have

strong student participation and public access to scientific findings using NCAR and University Web-based educational tools.

The COSMO facility will be designed, built, and operated by HAO/NCAR in collaboration with the University of Hawaii and the University of Michigan. It will replace the current Mauna Loa Solar Observatory, which has been collecting synoptic coronal data for over 40 years in support of the solar and heliospheric community (see Appendix 9.2). The design, development, and fabrication cost is estimated to be $22.6M. The planned schedule is for a completion time of five years, including a one-year Phase-B study. For continuing operations, NCAR will transfer the current facility budget of approximately $1.2M/year from the existing Mauna Loa Solar Observatory to the new COSMO facility, greatly reducing the recurring operational cost increment to NSF, which is estimated to be the addition of 1 FTE for data management, or approximately $200K/year.

2 SCIENTIFIC GOALS

The Sun is the primary source of energy to the Earth, and its output determines the conditions in the solar wind and throughout interplanetary space. The Earth's magnetic field and associated current systems react to changing conditions in the solar wind, which in turn are driven by processes occurring at the Sun. The continual eruption of magnetic flux into the solar atmosphere gives rise to various forms of solar activity. This activity can drive radical changes in the solar wind, creating disturbances in interplanetary space known as space weather. The evolving solar magnetic field drives most of the solar activity responsible for space weather disturbances, including high-energy electromagnetic radiation (EUV, X-ray, γ-ray), solar energetic particles (SEPs), flares, and coronal mass ejections (CMEs). Our primary scientific goal is to understand the magnetic structure of the Sun and how changes in the solar magnetic field impact conditions at Earth.

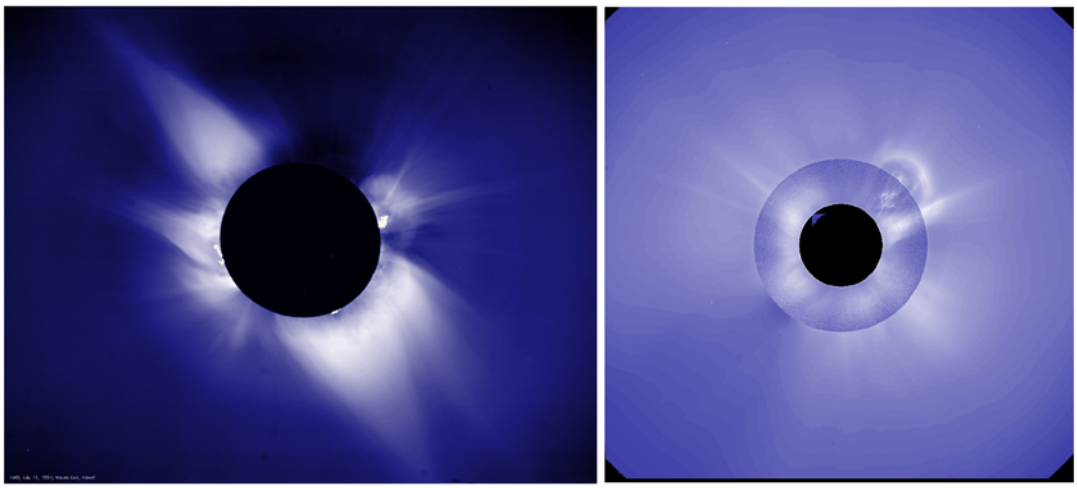

Figure 1 [left] An image of the solar corona taken during a total eclipse in 1991 by the HAO/NCAR eclipse team. Bright structures are regions where the coronal plasma is "held down" by the magnetic field (magnetically closed). Darker regions, known as coronal holes (e.g. near top of photo), are locations where the plasma escapes to form the solar wind (magnetically open). [right] A composite image of a coronal mass ejection on February 18, 2003. The inner corona was recorded by the MK4 coronameter at Mauna Loa, Hawaii and the outer corona was photographed from space by the LASCO C2 coronagraph onboard the SOHO satellite.

2.1 Importance of the Coronal Magnetic Field

The magnetic field dominates the energy balance in the outermost solar atmosphere, known as the corona, which is the source of the solar wind and most space-weather disturbances. The corona is a fully-ionized, million-degree plasma, which is an excellent conductor of electricity. This plasma is organized by the coronal magnetic field into two types of structures: (1) *magnetically closed* structures where magnetic forces act with gravity to contain the plasma, increasing the density and therefore the brightness of the region; and (2) *magnetically open* structures where the coronal plasma escapes the solar gravitational field to form the solar wind, producing low-density, dark regions known as coronal holes (see Figure 1).

The magnetic topology in the corona is continually changing in response to magnetic flux emerging from the solar interior through the photosphere. New cycle flux from the interior reverses the global solar magnetic polarity roughly once every 11 years (solar cycle). On the same time scale, the corona must process new and preexisting magnetic flux to totally reconfigure itself. Observations show that this occurs through a series of physical processes that are universal in astrophysics, yet poorly understood (see review by Low, 1994 and references therein). Free magnetic energy in coronal current systems can drive the heating and dynamics of the corona. This heating can be both quiescent and explosive in nature. During solar flares, explosive plasma heating leads to large perturbations in solar radiation, most obvious in bursts of radio, EUV, X-ray, and γ-ray emission. The strongest flares are frequently associated with large releases of magnetic energy stored in the magnetically closed corona when large volumes and masses of coronal plasma are suddenly ejected into space as a coronal mass ejection (CME).

It is important to note that some 75% of CMEs are associated with the eruption of cooler plasma in structures known as prominences (Hundhausen 1999). It has been suggested that CMEs are an essential component of the solar dynamo, as a necessary sink of magnetic helicity (Low 1994). Furthermore, CMEs are an important component of space weather, being the primary driver of large geomagnetic storms. CMEs and flares also accelerate high-energy particles, which pose hazards to astronauts and space-based technologies such as GPS systems, and to high frequency communications, power grids, and other vulnerable technologies on Earth (Lanzerotti, et al. 1998; Hanslmeier 2003; Lambour, et al. 2003; Iucci, et al. 2006; Zolesi and Cander 2006).

Because space weather events are driven by changes in the coronal magnetic field, understanding these changes could lead to predictions of their hazardous effects (1–4 days in advance). The rationale for studying coronal magnetic fields is compelling since the corona is the best laboratory available for studying basic magnetohydrodynamics (MHD) and plasma processes in a magnetically dominated system. Measurements in the corona can contribute to our understanding and prediction of space environment conditions at Earth.

The scientific community recognizes the critical need for observations of the coronal magnetic field. A call for better understanding of the solar atmosphere and the magnetic field was one of the top scientific priorities reported by the most recent National Research Council decadal review of research strategy in solar and space physics (Lanzerotti 2003). Specifically, the panel identified three questions:

(1) What physical processes are responsible for coronal heating and solar wind acceleration, and what controls the development and evolution of the solar wind in the innermost heliosphere?

(2) What determines the magnetic structure of the Sun and its evolution in time, and what physical processes determine how and where magnetic flux emerges from beneath the photosphere?

(3) What is the physics behind events of explosive energy release in the solar atmosphere, and how do the resulting heliospheric disturbances evolve in space and time?

Coronal magnetic field observations are essential to addressing the most important questions in solar physics. Yet until recently, magnetic fields in the corona have been extremely difficult to measure for three important reasons:

(1) *Weak fields*: The magnetic fields in the corona are intrinsically weak, making coronal field measurements difficult.

(2) *Faint, broad emissions*: The coronal spectroscopic lines are dimmer and broader than their photospheric counterparts.

(3) *Line-of-sight deconvolution*: The optically thin corona requires interpretation of magnetic signatures integrated along large path lengths, unlike photospheric signatures, which form over only a few hundred kilometers.

These challenges have been addressed in recent experiments using greatly improved infrared (IR) detectors, advanced modeling tools, and inversion codes. We have the most important opportunity in decades to observe coronal magnetic fields at scientifically useful spatial and temporal resolutions. Coronal magnetic field observations will provide information necessary for useful long-term predictions of space weather and will contribute to breakthrough advances in solar, heliospheric, and space-weather research. However, today's solar telescopes are too small for making the measurements we need at the necessary resolutions.

In this document, we propose to exploit the opportunity to observe coronal magnetic fields by creating the new COronal Solar Magnetism Observatory (COSMO). With this novel, multi-institutional, ground-based facility the anticipated breakthrough observations can be obtained and used to address some of the fundamental physical questions facing coronal physics. These include issues of immediate and direct relevance to the solar, heliospheric, and space-weather communities. The COSMO facility and its proposed operation are described in detail in Section 3.

2.2 Measuring the Magnetic Field in the Corona

An overview (Judge, et al. 2001) of methods for measuring coronal magnetic fields identified four promising techniques to infer magnetic information from the radiation emitted by coronal and prominence plasma, and thus to measure coronal magnetic fields by remote sensing. Two of these techniques apply to the radio domain of the solar radiation, and they are limited to strong magnetic fields (hundreds of Gauss) found above active regions (Bastian 2004). These radio techniques are not considered here. Instead, we focus on the two techniques that are capable of detecting both strong and weak coronal magnetic fields. These techniques apply to the optical and IR domain of the solar spectrum and are:

- The Zeeman effect and scattering polarization signatures of magnetic fields in forbidden (magnetic dipole) coronal emission lines
- Hanle depolarization of permitted transitions in coronal atomic ions and in strong lines in prominence plasmas

Zeeman effect and scattering polarization

The application of the Zeeman effect and scattering polarization to determine properties of the corona was pioneered in the 1960s (Charvin 1965; Hyder 1965; Perche 1965; Harvey 1969). The line-of-sight (LOS; also referred to as *longitudinal)* strength of coronal magnetic fields can be measured directly through the Zeeman effect, which is responsible for the circular polarization of coronal emission lines (Stokes *V*; see Figure 2). Judge et al. (2001) evaluated the available lines in the visible and IR regions of the spectrum and computed an expected precision for coronal magnetic field measurements based on the intensity, background level, and Zeeman

sensitivity of the various lines. Not surprisingly, owing to the wavelength-squared dependence of the Zeeman effect, the most promising lines are located in the IR region of the solar spectrum. Because the corona is optically thin at these wavelengths, on-disk observations are dominated by the IR emission of the chromosphere. Therefore, the IR corona can only be observed off-limb with coronagraphs (or at eclipses). For the same reason, LOS integration issues also arise in data interpretation (see Section 5.3).

The Zeeman effect can provide information on coronal magnetic fields with strengths as low as a fraction of a Gauss and as high as several thousand Gauss. This is extremely important in that it provides information on both the large-scale "quiet" coronal fields as well as the active region fields. The measurements are challenging because the circular polarization signal is very small: about 0.1% of the intensity for field strengths of 10 Gauss.

The plane-of-sky (POS; also referred to as *transverse*) direction of the magnetic field is determined directly from the linear polarization signals (Stokes Q and U; see Figure 2) of the scattered radiation, subject to a 90˚ ambiguity. This ambiguity is due to the "Van Vleck" effect, which causes nulls of linear polarization to occur at a specific angle between the magnetic field and the solar vertical. On either side of the null, the polarization direction changes by 90˚. Identification of nulls can then be used to tightly constrain the morphology of the magnetic structure.

We must note that the linear polarization of the IR forbidden lines is insensitive to the field strength, therefore the full vector magnetic field cannot be measured directly. However, measurements using the Zeeman effect and scattering polarization can yield full vector field information when the polarized light originates from a confined and localizable volume. In those cases, constraints can be placed on the inclination of the magnetic field and therefore the total field strength and direction. These issues are discussed in an upcoming publication (Judge 2007). Below we will see that recently identified Alfvén modes can be used to further constrain the magnetic field (see Sections 2.4 and 5.2). To overcome inherent limitations of LOS integrations and determine the 3-D structure of the magnetic field, a variety of models will also be used in conjunction with COSMO observations (see Section 5.3). More information on determining the magnetic field and plasma conditions from forbidden emission lines can be found in the literature (House 1977; Sahal-Bréchot 1977; Querfeld 1982; Casini and Judge 1999; Lin, Penn and Tomczyk 2000; Judge, et al. 2001; Lin, Kuhn and Coulter 2004; Judge, Low and Casini 2006).

Hanle effect

Hanle-effect measurements can be made at visible and IR wavelengths using permitted (electric dipole) transitions in cooler plasma—such as the chromosphere—and are essential for magnetic diagnostics of prominences and filaments. Advantages of these measurements over the Zeeman and scattering polarization measurements in the corona include the following: They can be made with or without coronagraphs; all states of polarization (Q,U,V) are sensitive to *both* strength and geometry of the magnetic field; the lines are at least an order of magnitude brighter, and being formed in cooler plasma the line widths are much narrower. Disadvantages include difficulties in dealing with radiative transfer effects if the lines are optically thick and in handling the influence of particle collisions in the theoretical formalism.

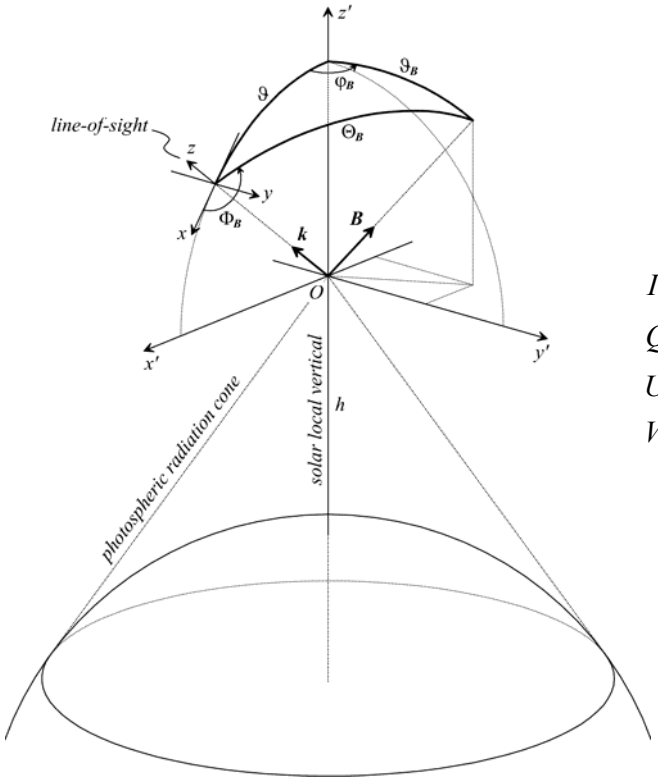

$$I(\omega) \propto [1 + a\sigma(\cos^2\Theta_B - \tfrac{1}{3})]\ \varphi(\omega - \omega_0)$$
$$Q(\omega) \propto a\sigma\ \sin^2\Theta_B \cos 2\Phi_B\ \varphi(\omega - \omega_0)$$
$$U(\omega) \propto a\sigma\ \sin^2\Theta_B \sin 2\Phi_B\ \varphi(\omega - \omega_0)$$
$$V(\omega) \propto (g + b\sigma)\, B \cos\Theta_B\ \varphi'(\omega - \omega_0)$$

Figure 2 Illustration of the magnetic geometry in the corona and how it relates to the polarized radiation observables (Stokes parameters: *I, Q, U, V*). In the formulae (Casini and Judge 1999): Θ_B and Φ_B are the inclination and azimuth of the magnetic field with respect to the LOS; a and b are atomic constants depending on the spectral line (for Fe XIII 1074.7 nm, a=1 and b=1/√2); σ is the so-called "atomic alignment" which depends on radiation anisotropy (through h), magnetic field (through ϑ_B), and plasma collisions; and *g* is the Landé factor of the line (for Fe XIII 1074.7 nm, *g*=1.5). Finally $\varphi(\omega-\omega_0)$ is the line profile centered at the line frequency ω_0.

We believe that despite the difficulties associated with these techniques, recent advances on both observational and theoretical fronts indicate that these techniques are ready to be fully exploited. Using them we can obtain unique information about coronal magnetic fields, which are critical for progress in solar and heliospheric physics.

2.3 Providing Answers about Coronal Processes

New solar observations acquired over the past three decades from increasingly sophisticated instruments on the ground and in space, have radically changed our view of the Sun. However, until relatively recently, attempts at measuring coronal magnetic fields have been unsuccessful, even while vector magnetic fields in the photosphere have been routinely observed via the Zeeman effect, with ever-increasing spatial, spectral, and temporal resolution.

The COronal Solar Magnetism Observatory (COSMO) will address a number of important questions that require knowledge of the coronal magnetic field. These research questions are illustrated in Figure 3.

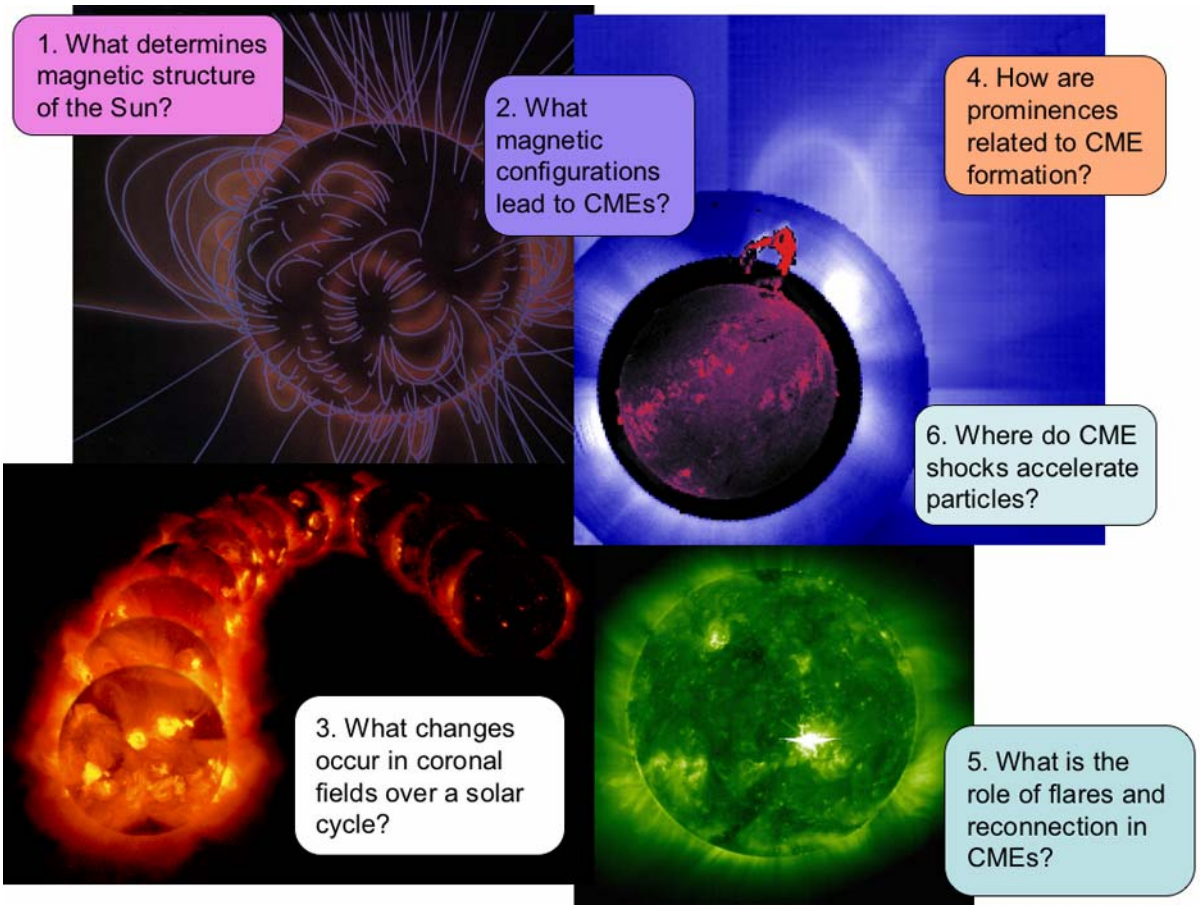

Figure 3 This set of images summarizes the six science questions to be addressed by COSMO.

(1) What determines the magnetic structure of the Sun?

And how does it evolve over time? How does magnetic flux emerging from beneath the photosphere impact coronal energy balance and dynamical stability? What physical processes are responsible for coronal heating?

The corona must adjust to the continual emergence of magnetic flux through the photosphere that is ultimately driven by the solar dynamo. COSMO observations of coronal magnetic fields will provide information on rapid changes in local conditions resulting from processes such as flux emergence and magnetic reconnection. Observations will also reveal evolutionary changes from global processes, such as surface field advection and differential rotation. COSMO will also measure the magnetic field in the chromosphere, providing crucial boundary information between the corona and the photosphere. COSMO observations are needed to validate coronal models derived from photospheric magnetic field measurements. The current lack of coronal magnetic field observations is unsatisfactory, because the majority of studies must resort to comparisons of models or extrapolation of magnetic fields using only the morphology of X-ray or EUV plasma loops (for example, see Longcope et al. 2001).

Coronal seismology techniques will also be pursued with COSMO. As discussed in section 2.4, a COSMO prototype instrument (Tomczyk et al., 2007) has demonstrated a method to detect Alfvén waves in the corona. These MHD waves are an important tool for determining how the corona is heated and the solar wind is accelerated. COSMO will record Alfvén wave

properties in order to probe the structure of magnetic fields, identify their importance in heating the corona, and provide a measure of important quantities, such as twist and writhe, which define the helicity and free energy content of the corona.

(2) What magnetic configurations lead to coronal mass ejections (CME)?
What leads to the launch and acceleration of CMEs?

CMEs form under a wide variety of coronal conditions throughout the solar cycle, therefore, long-term, routine coronal magnetic field observations are needed to establish their causes. In particular, these observations will directly address question 3 from the decadal review of research strategy in solar and space physics (Lanzerotti 2003) regarding explosive energy releases in the solar atmosphere. While it is generally agreed that CMEs derive their energy from coronal magnetic fields (see review by Forbes 2000 and references therein), the question of which magnetic configurations lead to their formation remains unknown. The topic has been explored through modeling efforts that rely on extrapolations of the coronal field from photospheric observations and inferences of coronal field structure from morphological studies using intensity images. While these modeling efforts have led to advances in our understanding of CMEs, they remain of limited use due to the fact that field extrapolations and inferences are insufficient to constrain and discriminate between the models. COSMO observations will define pre-CME configuration, and the success or failure of the various models will be evident for the first time. COSMO will provide an unprecedented combination of magnetic field and plasma observations in the corona and chromosphere. It will also provide rapid time sequences of white light images of CMEs in the very low corona in the earliest stages of CME development.

(3) What changes occur in coronal fields over a solar cycle?
What kinds of changes in coronal magnetic structure accompany the 11-year solar cycle and the reversal of magnetic polarity? How is this reflected in the development and evolution of the inner heliosphere? Do CMEs play a vital role in relieving the Sun of its accumulated magnetic helicity that arises from the large-scale dynamo?

At present, the only coronal data covering solar cycle time scales consists of EUV, X-ray, and white-light or emission-line intensity data. The behavior of the white-light and emission-line corona relative to the sunspot cycle has been long known (Van de Hulst 1953), and the SOHO and TRACE spacecraft have provided data covering 11 years. While the intensity data have proven useful as qualitative indicators of the coronal field morphology, they lack the necessary quantitative magnetic information to properly characterize the three-dimensional field, its free-energy content, and its evolution. Spacecraft have, to some degree, determined the cycle variability of conditions far out in the solar wind, but very little is known concerning the magnetic fields; we are severely constrained in our understanding of how the coronal field responds to the sunspot cycle. In particular, we have no idea how the switch in polarity of the global (poloidal) field manifests itself in the heliosphere. Long-term synoptic observations of the coronal magnetic field will directly address this critical question. Understanding the basic nature of the solar magnetic environment will lead to a better understanding of solar variability. Needless to say, the question of magnetic helicity is left unanswered until magnetic field measurements can be made. This open question is particularly pressing because, if CMEs are important sinks of helicity, then they play a fundamental role within the hydromagnetic system and in the Sun's cyclic dynamo mechanism (Low 1994). Addressing the relationship between coronal magnetic fields and the sunspot cycle is a major goal of the COSMO project.

Observations with a large field-of-view (FOV) and sufficient angular resolution are required to constrain helicity.

(4) How are prominences related to CME formation?

How are prominences formed, how do they evolve, and how are they related dynamically to CMEs?

Since prominences are strongly associated with the eruption of CMEs, this question also relates directly to question 3 from the decadal review of research strategy in solar and space physics (Lanzerotti 2003). Prominences provide physical information on the hydromagnetic environment in the corona where CMEs originate and they may play a critical role in CME formation. Prominences are cool, dense plasma structures seen in emission when they appear above the solar limb and in absorption when viewed against the solar disk (where they are known as filaments). Prominences interact with the magnetic field in ways that support the plasma against gravity and thermally insulate it from the surrounding million-degree corona. Despite the fact that most CMEs are associated with active and erupting prominences (Low 2001; Schmieder, et al. 2002), vector magnetic field observations in prominences ceased in the mid-1980s and have only recently been acquired again (Paletou, et al. 2001; Trujillo Bueno, et al. 2002; Casini, et al. 2003). Prominence vector magnetic field observations have established two hydromagnetic configurations of prominences and surrounding coronal magnetic fields, known as normal and inverse (Leroy, Bommier, and Sahal-Bréchot 1984; Bommier, et al. 1994). A recent model (Low and Zhang 2002; 2004) provides a physical basis for the rapid acceleration of the fastest CMEs based on the magnetic configuration of normal prominences. Yet there are no direct magnetic observations to support or reject this or other models of CME acceleration. COSMO will provide routine observations of prominence (limb) and filament (disk) magnetic fields along with prominence flows and constraints on prominence densities. This information can be used to determine the structure and evolution of prominences and their role in CME formation. COSMO observations of the magnetic field in the chromosphere will be essential for augmenting the signatures predicted in the surrounding corona (Judge, Low and Casini 2006).

(5) What is the role of flares and reconnection in CMEs?

What is the role of magnetic reconnection in flares and CME initiation? How does the magnetic field change around flare sites?

Flares are perhaps the most recognizable form of explosive energy release in the solar atmosphere. It has long been known that many CMEs are accompanied by X-ray and EUV flares, especially flares of long duration and high intensity (Sheeley, et al. 1983). Recent work suggests that the impulsive stages of flares occur during times of CME acceleration (Zhang, et al. 2001; Alexander, Metcalf and Nitta 2002; Zhang, et al. 2004) but how these phenomena are related is still undetermined and remains controversial (Gosling 1993; Gosling and Hundhausen 1995; Svestka 1995). Magnetic reconnection plays a central role in the energy release responsible for solar flares and may be a critical component in the formation, development, and coronal response to a CME. Whether reconnection is a requirement for CME initiation or a response to the coronal destabilization caused by a CME is still under considerable debate. Understanding the role of magnetic reconnection in the production of flares and CMEs and determining how magnetic fields evolve prior to and following magnetic reconnection is of fundamental importance to the solar, terrestrial, and astrophysical communities, since the process of magnetic reconnection is universal in plasmas. To establish the relationship between CMEs,

flares, and magnetic reconnection, COSMO will provide the first measurements of coronal magnetic fields in the source regions that spawn flares and CMEs.

(6) Where do CME shocks accelerate particles?

How and where are particles accelerated to high energies? Where are CME-associated shocks formed in the corona, and what is their role in the production of solar energetic particle events?

Solar energetic particles are the product of explosive energy releases in the solar atmosphere. Observations suggest that there are, roughly speaking, two phenomena that produce solar energetic particle events (SEPs): flares and CME-associated shock waves. Particles accelerated by CME-driven shock have the highest particle energies and pose the greatest space-weather hazards. Recent observations suggest that at least some shocks responsible for SEP events form low (below 2.5 R_{sun}) in the solar corona (Ciaravella, et al. 2005), where densities are significantly higher, and the shock has access to a large population of particles.

How particles are accelerated and transported at and around shocks is complex and not well understood. With the exception of γ-ray emission, direct detection of the acceleration sites of shock-induced SEPs has not been possible, since most of the particles are accelerated in regions of such low densities that no detectable photon intensities are produced. However, the density compressions resulting from shock formation can be large enough to produce intensity enhancements in white-light and chromospheric emission images so that the shock itself can be detected and tracked (Sime and Hundhausen 1987; Vourlidas, et al. 2003). To detect rapid changes, such as shock waves, in the early stages of their formation, COSMO will provide the highest time cadence (~15 seconds) of white-light imagery of the very low corona (down to 1.05 R_{sun}). COSMO observations can be used to detect compressions and distortions in the field due to the formation and passage of a CME and associated waves. This information can advance modeling efforts necessary to fully understand particle acceleration.

COSMO's first-of-a-kind observations will contribute significantly to answering these, as well as other important questions about solar processes, in particular, coronal heating. While heating mechanisms are believed to require small-scale structures more properly observed with the ATST, COSMO will complement ATST observations by identifying wave motions, for example. These essential observations are not provided by any current or proposed ground- or space-based mission.

2.4 Prototype Science Results

Prototype instruments are producing results that, although limited by small aperture, illustrate the potential and feasibility of COSMO to greatly enhance coronal, heliospheric, and space-weather research. One prototype, the University of Hawaii Solar-C, 46-cm aperture coronagraph (Kuhn, et al. 2003) at Haleakala, is shown in Figure 4. It records the intensity and the linear and circular polarization (Stokes *I,Q,U,V*) of the forbidden line of Fe XIII at 1074.7 nm. This emission line has greater magnetic sensitivity than the green coronal line at 530.3 nm employed by Harvey (1969). These IR observations were made possible by the recent availability of high quantum efficiency, low-noise, IR array detectors.

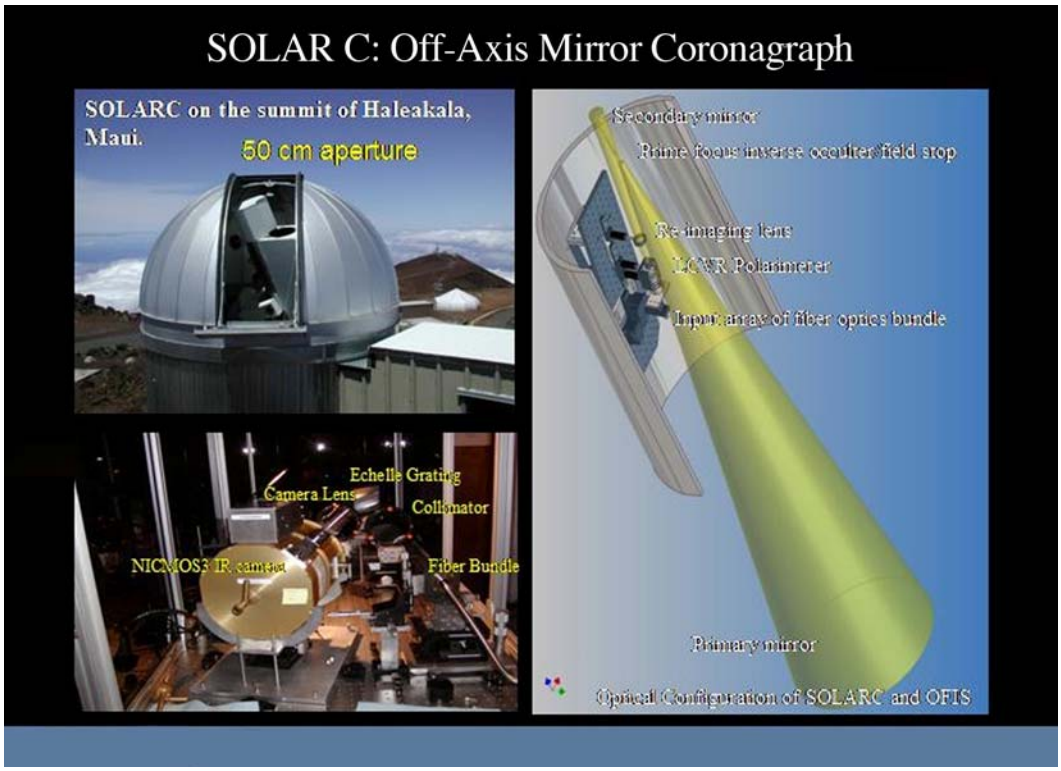

Figure 4 [upper left] The University of Hawaii Solar-C telescope at Haleakala. [right] An illustration of the telescope design. [lower left] A photograph of the fiber-fed spectrograph.

Figure 5 shows recent measurements (Lin, Kuhn and Coulter 2004) of the POS direction of the magnetic field (on the left) and the LOS strength (on the right). The observations were obtained with a fiber-fed spectrograph, the Optical Fiberbundle Imaging Spectropolarimeter (OFIS), behind Solar-C.

The fiber bundle subtended 20 arcsec and the observation required 70 minutes of integration time. Notably, the errors on the LOS component of the magnetic field are less than 1 Gauss. The precision on the magnetic field achieved with this instrument demonstrates that the technique is sufficient to address some of the science goals of the community. However, the limited FOV and the coarse spatial and temporal samplings are not sufficient to address the six science questions posed in Section 2.3 above. More photons are needed to achieve the required noise levels at scientifically interesting spatial and temporal scales as discussed below. This can only be accomplished with a larger-aperture coronagraph.

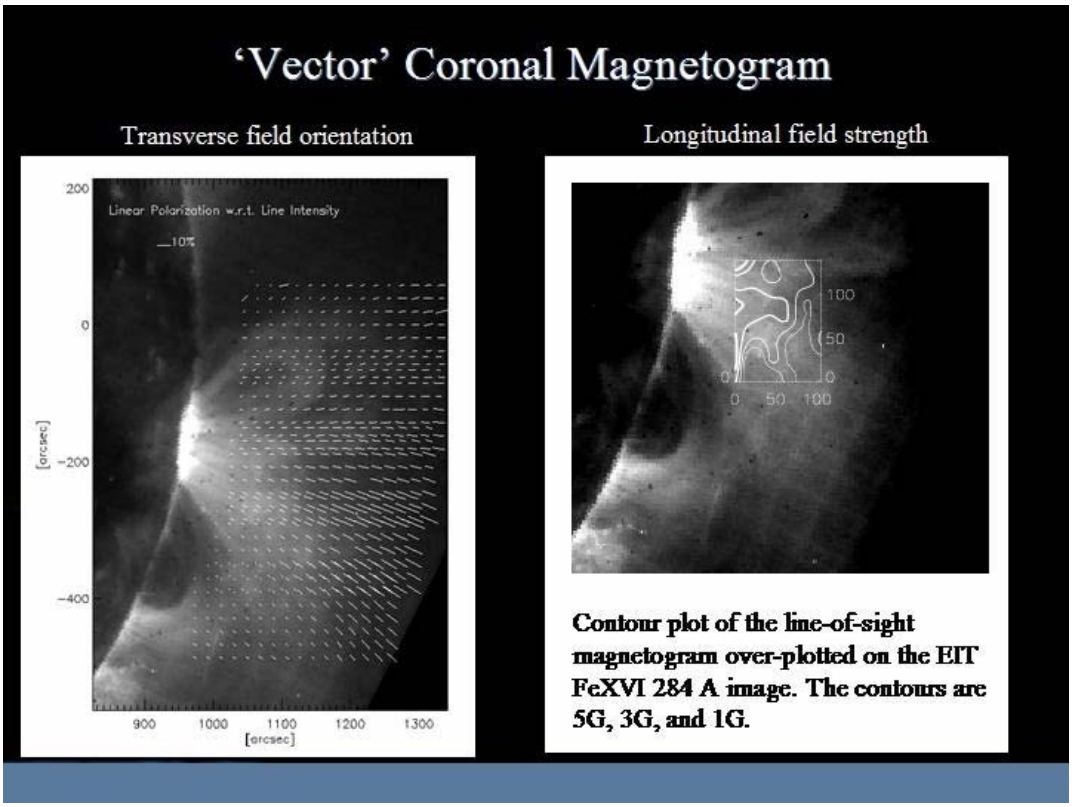

Figure 5 Coronal magnetic field observations from Solar-C and the EIT instrument. At left is the direction of the magnetic field onto the POS, derived from linear polarization measurements and superposed on EIT instrument observations. At right is a contour plot of the LOS magnetic field strength determined from circular polarization and superposed on EIT observations for context.

Another application of this technique and the use of new IR detector technology are illustrated in Figure 6. This shows coronal properties measured by Tomczyk and co-workers in April of 2005, using the HAO/NCAR Coronal Multi-channel Polarimeter (CoMP) on the 20-cm aperture OneShot coronagraph at NSO's Sacramento Peak Observatory in New Mexico. The CoMP instrument (Tomczyk et al., 2007) can observe the coronal magnetic field (POS field direction and LOS field strength) with a full view of the low corona (~1.03 to 1.5 R_{sun}), as well as obtain information about the plasma density and motion. Like Solar-C, CoMP records the full Stokes vector (*I,Q,U,V*) of the forbidden lines of Fe XIII at 1074.7 nm and 1079.8 nm. The LOS plasma velocity is measured from Doppler observations in the wings of the line intensity (Stokes *I*), and the LOS column density from the ratio of the lines at 1074.7 and 1079.8 nm.

These observations have a spatial sampling of 4.5 arcsec/pixel and required 30 minutes of integration time to attain a measure of the LOS magnetic field strength. The LOS field strength measurements shown at lower right in Figure 6 are significantly worse than those shown in the Solar-C data due to the smaller coronagraph aperture (20 cm vs. 46 cm on Solar-C), shorter integration time, and smaller pixel size. To meet the science requirements discussed in Section 2.6, a large-aperture coronagraph is needed.

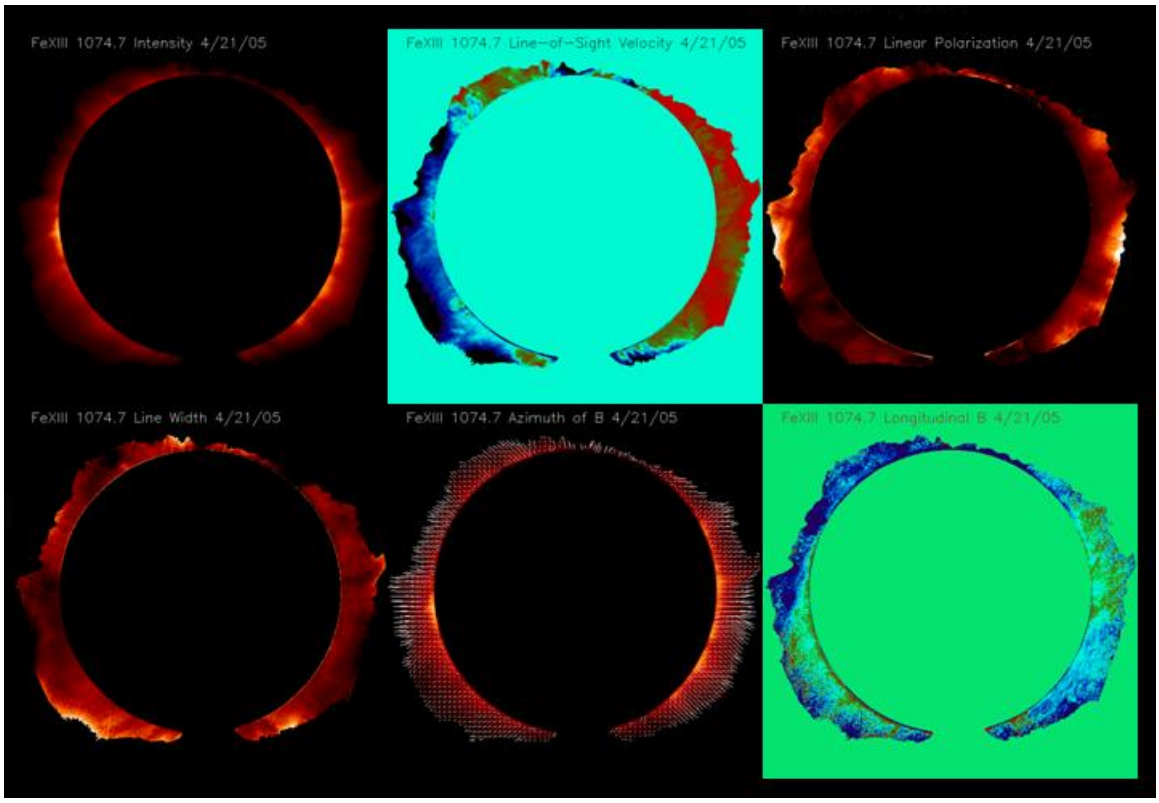

Figure 6 Clockwise from top left: the intensity, velocity, degree of linear polarization, LOS magnetic field, field azimuth, and line-width as observed by the CoMP instrument on 4/21/05.

Despite the limited aperture, CoMP observations reveal ubiquitous propagating 3-5 mHz fluctuations in the solar corona, which have been identified as being predominately Alfvénic (Tomczyk, et al. 2007) in nature. This remarkable observation of MHD waves in the corona is possible due to the combined measurements of LOS velocity and linear polarization over a wide range of coronal heights (see Figure 7) with very high time cadence (29 seconds). Phase travel-time analysis (Jefferies, et al. 1994; Jefferies, et al. 1997; Finsterle, et al. 2004; McIntosh, Fleck and Tarbell 2004) was used to detect the Alfvén waves in CoMP velocity observations. Furthermore, it was possible to estimate that the resolved fluctuations fall far short of providing the primary source of energy needed to heat the corona. The detection of Alfvén waves in the corona provides important insights on the processes responsible for coronal heating. We will build upon this result with more sophisticated observations of coronal waves from the large-aperture COSMO coronagraph to explore both the magnetic and plasma structure of the corona.

These exciting discoveries are but one example of the breakthrough science that is possible with COSMO, and they clearly demonstrate the potential of these observational techniques. However, these prototype results are severely limited by the modest apertures of the available coronagraphs. The aperture size needed to properly address COSMO scientific goals is determined by examining the observational requirements.

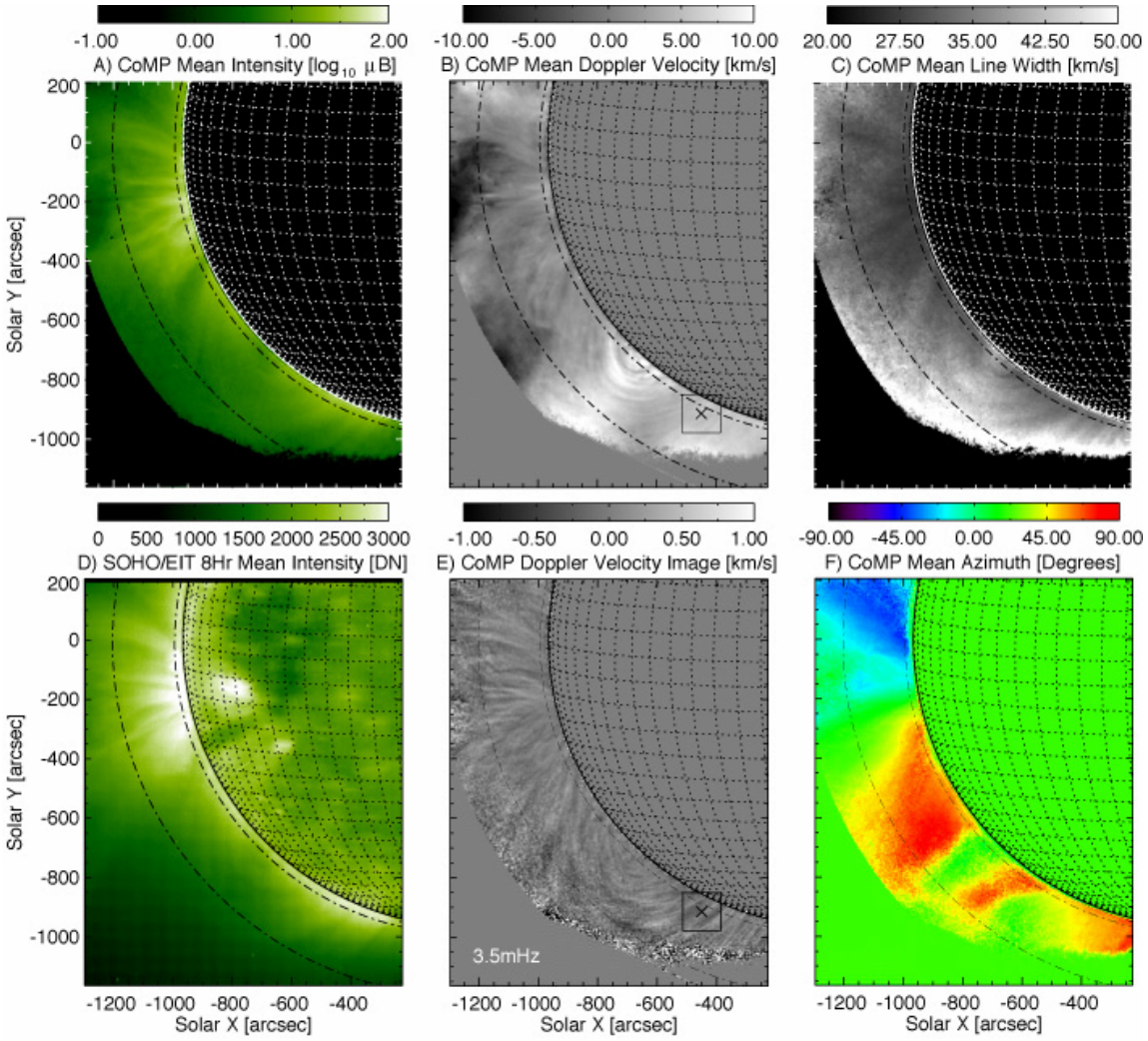

Figure 7 CoMP observations of the solar corona in October 2005. CoMP has a spatial sampling of 4.5 arcsec/pixel. The inclusion of LOS velocity measurements, along with intensity and linear polarization, reveal ubiquitous propagating 3-5 mHz fluctuations in the solar corona, which have been identified as being predominantly Alfvénic (Tomczyk, et al. 2007).

2.5 Observation and Telescope Requirements

The goal of the COSMO facility is to provide the observations needed to address the six key science questions posed in Section 2.3 above and enumerated here:

(1) What determines the magnetic structure of the Sun?
(2) What magnetic configurations lead to CMEs?
(3) What changes occur in coronal magnetic fields over a solar cycle?
(4) How are prominences related to CME formation?
(5) What is the role of flares and reconnection in CMEs?
(6) Where do CME shocks accelerate particles?

Table 1 COSMO Requirements

Science Objective	Key Predictions	Observation Requirements	Telescope Requirements				
			Intensity Range (μB brightness of solar disk)	**Field Sensitivity** (Gauss)	**Spatial Resolution** (Arcseconds)	**Temporal Resolution** (Minutes)	**Other Requirements**
1. Determine magnetic structure of corona and how it relates to photospheric magnetic fields	Determine validity of potential and force-free models of coronal magnetic field from photospheric field extrapolations. Estimate the distribution of magnetic free energy in the corona.	Measure magnetic field at all latitudes	Observe coronal structures down to 0.5	1-2	5	30	Large FOV (3 R_{sun} x 3 R_{sun}), observe at lowest heights possible
2. Identify magnetic configurations that lead to CMEs	Determine role of twist and writhe in CME production; identify magnetic structure of CME for space-weather forecasting	Measure magnetic field in corona and prominences and polarization brightness (pB)		1-2	5	< 1 Stokes (*I*,*Q*,*U*) and pB; 10 Stokes (*V*)	Large FOV, observe at lowest heights possible
3. Understand the nature of changes in the global coronal magnetic field over the 11-year solar cycle	Determine how magnetic fields reverse polarity over the solar cycle and how helicity is shed to permit this reversal	Measure magnetic field at all latitudes. Dedicated instrument to provide long time series of observations	Observe coronal structures down to 0.5	1-2	5 To determine constraints on helicity	30	Large FOV, observe at lowest heights possible
4. Determine how prominences form and relate to CMEs	Determine when flux ropes form to test prominence models; identify normal vs. inverse magnetic fields in models to test theories	Measure prominence fields using optical and IR emission lines and pB		1-2	2	10-20	Large FOV, small pixels to determine constraints on helicity
5. Understand the role of flares and magnetic reconnection in CME formation	Test breakout, tether-cutting, and flux rope models of CMEs	Measure magnetic field and polarization brightness (pB)		1-2	3-5	< 1 Stokes (*I*,*Q*,*U*) and pB; 10 Stokes (*V*)	Large FOV, observe at lowest heights possible
6. Identify CME shocks in the corona	Determine how strength of particle events relates to height of shock formation	Measure magnetic field and polarization brightness (pB)	Observe coronal structures down to 0.5	1-2	3-5	< 1 Stokes (*I*,*Q*,*U*) and pB; 10 Stokes (*V*)	Large FOV

Table 1 Summary of COSMO science objectives and requirements. We have included a list of key predictions that COSMO will provide to the community. Note that only the strictest intensity ranges are noted in the telescope requirement section.

These questions, identified by the COSMO science advisory panel and the Principal Investigators and their teams, have been translated into observational and telescope requirements, as summarized in Table 1. Science questions 1 and 3 require observations of the coronal magnetic field at all latitudes on the Sun to determine its global properties. The Fe XIII lines at 1074.7 nm and 1079.8 nm were chosen for COSMO for reasons of line intensity, and sensitivity to coronal magnetic fields from a fraction of a G to thousands of G (Judge, et al. 2001).

The intensity sensitivity requirement for COSMO can be determined by examining the intensity of the 1074.7 nm line as a function of coronal height. Figure 8 shows that the brightest structures are located at low latitudes (< 25 degrees) where active regions exist. The faintest

structures are located at high latitudes (> 50 degrees). Faint, high-latitude regions are more difficult to detect but are critically important for determining how the global field reverses itself and how helicity is shed over the solar cycle. In addition, high-latitude regions often contain features known as coronal holes. They are the source of the fast solar wind and are therefore important for understanding the relationship between conditions in the corona and those of the inner heliosphere. In order to determine the magnetic field strength at all solar latitudes, COSMO will observe features down to 0.5 μB_{sun} (a millionth of the brightness of the solar disk).

In addition to measuring magnetic fields at coronal temperatures, we have also identified the need to measure the field in the chromosphere and in prominences (science question 4 above). Chromospheric observations provide important information on plasma conditions in the very low atmosphere that are needed to bridge observations of coronal magnetic fields with those measured at the surface. Measurements of prominence fields are rare but have been obtained using the Hanle effect as described in Section 2.2 above (Leroy 1981; Querfeld, et al. 1985; Bommier, et al. 1994; Paletou, et al. 2001; Casini, et al. 2003). This research has determined that the optimal lines for examining magnetic fields in prominences are the He I 587.6 and 1083.0-nm lines. These observations are ideally accomplished with a separate and smaller telescope to observe the chromosphere and prominences above the limb and on the disk.

The requirement for field strength sensitivity is set by estimates of coronal magnetic fields from extrapolations of photospheric fields. COSMO will be sensitive to magnetic field strengths of a few Gauss for the faintest coronal structures and less than a Gauss for bright structures.

Another requirement is to observe magnetic fields rapidly enough to detect and understand the dynamical processes responsible for CME production, prominence eruptions, magnetic reconnection, wave propagation, and shock formation. High time cadence is needed to satisfy science questions 2, 4, 5, and 6 above. These phenomena are associated with dynamical processes that can occur on time scales as short as a few seconds to a few minutes. Time scales of 30 minutes to an hour are sufficient for studying the evolution of large-scale coronal structures.

A large FOV is needed for observing the global structure of the corona and for measuring the properties of dynamic events such as CMEs. In addition, it is necessary to observe as low in the corona as possible in order understand how the corona continually reacts to changes occurring in the photosphere and chromosphere and to observe the formation of solar activity, which originates predominantly in the very low corona.

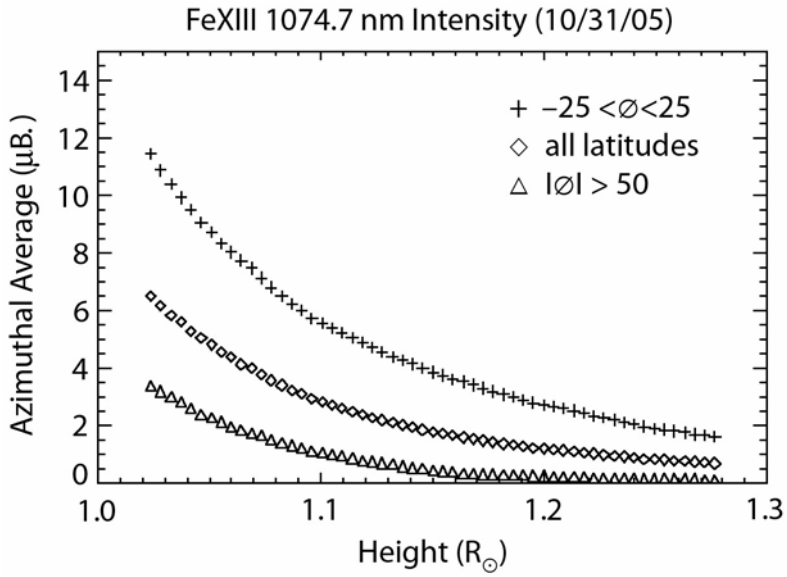

Figure 8 Average intensity of the corona in the Fe XIII emission line of 1074.7 nm for three latitude bins is shown as a function of height in the atmosphere, where height is measured in units of solar radii from Sun center. The intensity is plotted on the y-axis in units of a millionth of the brightness of the solar disk. Intensity falls off rapidly with height at all latitudes, due to the strong dependence of line intensity on coronal density. These measurements were taken by the CoMP instrument on October 31, 2005, and are independent of telescope aperture. Sky brightness has been removed from the observations.

The study of CMEs (science questions 2, 4, 5, and 6) requires additional information on the density structure of the corona over a larger FOV in order to track the outward motion and other basic properties of CMEs (and prominences) as they are ejected from the corona. While CMEs have been tracked in a variety of wavelengths, their basic properties are most easily determined in broadband white-light observations. Since the scattered light from the corona is partially polarized, it can be detected from the ground by observing polarization brightness with a broadband filter. Broadband filters acquire significantly more photons than narrowband filters, so that a small-aperture telescope can be used to acquire these observations.

Spatial resolution of 5 arcsec is sufficient for addressing many of the scientific questions pertaining to the large-scale magnetic structure of the Sun. Higher spatial resolution is needed (a few arcseconds) to resolve magnetic structure in prominences (science question 4), which are more highly structured due to their cooler temperatures (small-scale heights), and at reconnection sites and current sheets (science question 5).

We summarize the science objectives, observation requirements, and telescope requirements in Table 1. These objectives and requirements were designed by the COSMO science advisory panel (SAP) and the Principal Investigators and their teams based on current knowledge of coronal conditions and dynamics.

We conclude that the observational requirements can be met with three telescopes: one to measure coronal magnetic fields, one to measure the magnetic field in the chromosphere and in prominences, and one to measure the density structure of the corona and CMEs. These instruments are discussed in detail in Section 3. They combine state-of-the art and proven technologies, and they make maximum use of existing hardware and facilities to optimize performance while minimizing cost.

3 TECHNICAL IMPLEMENTATION

The proposed COSMO facility consists of two major elements: a large-aperture coronagraph with its own pointing system and dome, and a solar-pointed spar for the supporting instrumentation in a smaller adjacent dome. The large-aperture coronagraph is a 1.5-m aperture refractor with two accompanying instruments: a narrow-band tunable filter polarimeter for synoptic measurements, and a fiber-fed spectro-polarimeter for high-spectral-resolution observations. The supporting instruments are a white-light coronagraph to record the evolution of the electron scattered corona (K-corona), and a chromosphere and prominence magnetometer for disk and limb measurements of magnetic fields in the chromosphere and prominences using filter polarimetry. Conceptual sketches of the large-aperture coronagraph in its dome and the overall observatory facility are shown in Figures 9 and 17 respectively.

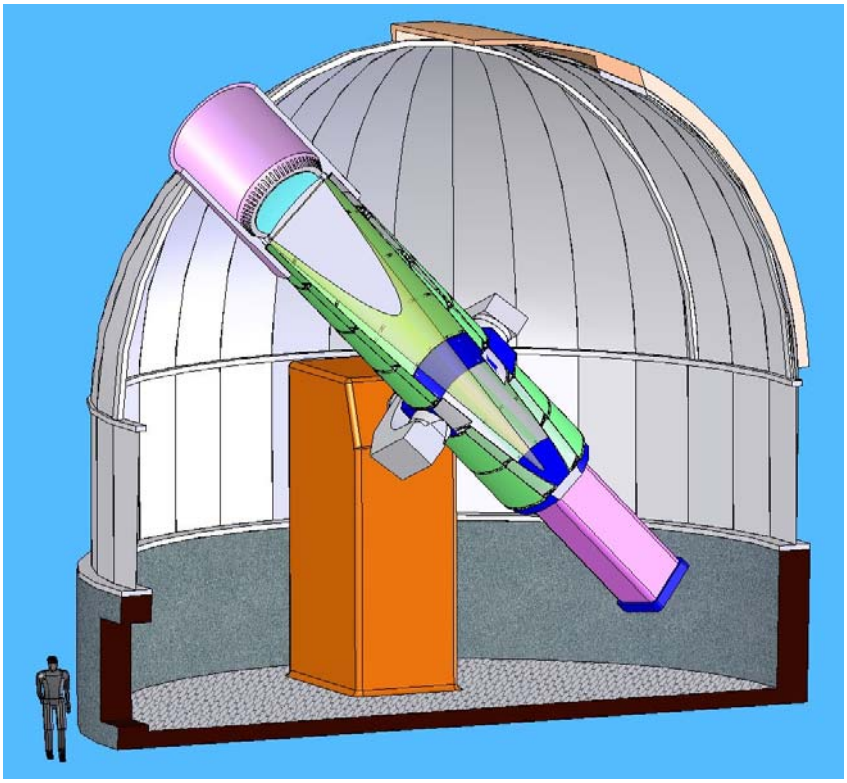

Figure 9 Concept for the COSMO coronagraph and dome. The telescope is a simple tube structure on an equatorial mount; the diameter of the dome is 12.2 m. The f/5 cone of light is shown in section. A protective "snout" extending through the telescope slot when the dome is open allows the lens to be continually washed in HEPA-cleaned air. The tube, sealed and filled with helium, completely protects the back surface of the lens from contamination and improves telescope seeing. The post-focus instrument package is 3 m long and contains relay optics, the filter magnetograph, and the pick-off for the fiber-fed spectrograph. The fiber-fed spectrograph will reside in another room.

3.1 Proposed Suite of Instruments

The most important instrument in the COSMO suite is a large-aperture coronagraph with instrumentation to measure coronal magnetic fields. However, in order to exploit coronal magnetic field measurements to their full potential for advancing science they should be

considered in the context of the ambient plasma environment. For this reason, crucial information on prominence magnetic fields and the dynamical conditions of the embedded plasma will be collected by two additional instruments: a white-light K-corona coronagraph and a chromosphere and prominence magnetometer. These additional supporting instruments are designed to provide temporal and spatial resolutions that meet or exceed the temporal and spatial resolutions of the coronal magnetic field observations from the large-aperture coronagraph.

This suite of instruments provides both the coronal magnetic field observations and the plasma environment context to achieve the science goals outlined in Table 1. A brief description of the three main instruments follows.

- *Large-aperture coronagraph.* This solar telescope (Figure 9) performs coronal magnetometry using the coronal forbidden emission lines of Fe XIII at 1074.7 and 1079.8 nm and the He I chromospheric emission line at 1083.0 nm. This coronagraph will have an aperture of 1.5 m and a full FOV of 1 degree. Post-focus instrumentation includes a *narrow band tunable filter* able to observe the entire FOV, as well as a *fiber-fed spectrograph* capable of high spectral resolution line profile observations.

- *White-light K-coronagraph.* This 20-cm aperture white-light coronagraph provides observations of CME formation and early acceleration. It replaces the 1970s-vintage Mauna Loa Mk4 system, the world's only ground-based white-light coronameter, with modern technology that allows observations with improved spatial resolution, temporal resolution, FOV, and signal-to-noise ratio. Given the absence of a white-light coronagraph on the SDO spacecraft, the K-coronagraph will be an essential complement to space- and ground-based coronal instruments.

- *Chromosphere and prominence magnetometer.* This supporting magnetometer is designed to observe the He I 587.6- and 1083-nm lines, and Hα, both on the solar disk and above the limb. This instrument, which we call "ChroMag," will have the ability to determine magnetic fields and LOS Doppler shifts.

3.1.1 The Large-aperture Coronagraph

The large-aperture coronagraph and associated magnetograph present design challenges owing to the faintness of coronal emission lines relative to the disk, their large thermal widths, and the weakness of coronal magnetic fields. The requirements for the COSMO large-aperture coronagraph and the impacts of these requirements on the design are discussed in detail here.

First, the requirement to observe close to the solar limb forces us to adopt an internally occulted design for the COSMO coronagraph that allows observations down to 1.02 R_{sun}. While externally occulted coronagraphs provide lower scattered light levels than the internally occulted type, the vignetting that naturally results in externally occulted coronagraphs would exclude observations very close to the solar limb.

The fractional amplitude of the Zeeman-induced circular polarization (Stokes *V*) signal, which constrains the strength of the LOS magnetic field, is about 10^{-3} for a 10 Gauss field for the Fe XIII 1074.7-nm line (Lin, Kuhn and Coulter 2004). The linear polarization signals, which provide information on the POS azimuth of the magnetic field, are typically much larger, on the

order of a few percent. This means that the aperture of the large coronagraph will be driven by the signal-to-noise requirement for the circular polarization measurements. The expected noise in the LOS component of the coronal field can be derived from considerations of the propagation of errors in the circular polarization measurements (Tomczyk 2006a), and is given by:

$$\sigma_B[\mathrm{G}] = \frac{8500}{\sqrt{I}}\sqrt{1+2\frac{B}{I}} \qquad [1]$$

where I and B are the number of photons in the emission line and background, respectively. This equation assumes photon noise limited observations in the Fe XIII 1074.7-nm (g=1.5) emission line. If many observations are taken in the continuum, as in spectrograph measurements, the factor of two in the term on the right approaches unity (Penn, et al. 2004). We can combine Equation 1 with a flux budget for the corona and compute the expected noise level as a function of coronagraph aperture size, coronal brightness, and background level. This is illustrated in Figure 10, assuming a system throughput of 5%, a spatial resolution of 5 arcsec, and integration times of 5 minutes (at left) and 30 minutes (at right). The plot on the left shows that a field sensitivity of less than 1 Gauss will be achieved in 5 minutes for coronal intensity greater than a few millionths of the intensity of the solar disk (μB_{sun}) for an aperture of 1.5 m and a background level of 5 μB_{sun}. However, in order to measure coronal magnetic fields in faint, high-latitude coronal structures with intensities of 0.5 μB_{sun} to meet science requirements discussed in Section 2.6, integration times of 30 minutes are required with a 1.5-m aperture, as shown in the plot at right in Figure 10.

We conclude that a 1.5-m aperture is sufficient to achieve the scientific requirements of the COSMO large coronagraph. The diffraction limit corresponding to an aperture this size is 0.18 arcsec at a wavelength of 1 μm, which is more than an order of magnitude smaller that the spatial resolution requirement for COSMO. This means that the COSMO coronagraph can operate as a "light bucket," far from the diffraction limit.

The sensitivity of the measurement to the background level through the term on the right side of Equation 1 implies that for background-limited observations, the noise in the magnetic field measurements will scale as the square root of the background level. The nature of noise propagation in background-limited observations results in a fundamental difficulty in the measurement of the magnetic fields for faint coronal features in the presence of significant background levels. Therefore, it is critically important that the COSMO large-aperture coronagraph be located at a site of exceptional quality for observing the corona and that the coronagraph be designed to ensure an extremely low level of instrument scattered light. Compared to a telescope like the ATST, the COSMO coronagraph requirements are shifted away from high spatial resolution toward large FOV and low scattered light.

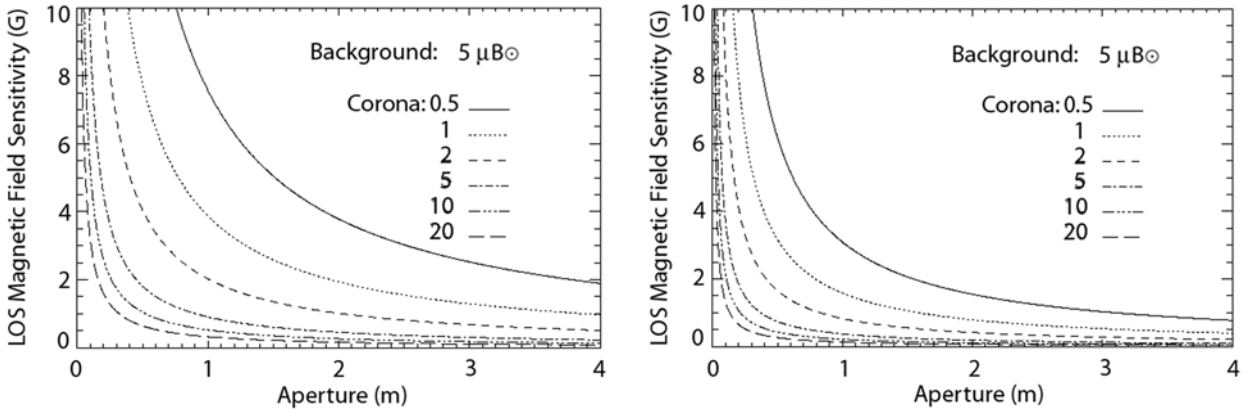

Figure 10 These plots illustrate the LOS magnetic field strength sensitivity using the FeXIII 1074.7-nm line vs. telescope aperture for two integration times: 5 minutes (at left) and 30 minutes (at right) assuming a sky brightness background of 5 μB_{sun}, which is a reasonable value for the pristine sky conditions available in Hawaii. The lines plotted correspond to various intensities of the corona in units of millionths of the disk intensity. It is possible to achieve magnetic field sensitivities of 1-2 Gauss (to meet scientific requirements) in 5 minutes for coronal structures with brightness of 2 μB_{sun} in the Fe XIII line of 1074.7 nm with a 1.5-m aperture telescope. Structures as faint as 0.5 μB_{sun} combined with field sensitivities of a few Gauss require a 1.5-m aperture for a 30 minute integration time (at right).

To identify the large-aperture coronagraph design that is best suited to the COSMO requirements, two designs were considered: a traditional refracting design using an uncoated fused silica singlet (f/5 to f/7) and an off-axis reflector (f/3 to f/5). The scattered light performance of these designs due to surface roughness, particulate contamination, and (in the case of refractors) imperfections of the glass was considered (Nelson 2006a). The primary tool used for these calculations was the Modeled Integrated Scatter Tool (MIST - v.2.10) developed by Thomas A. Germer at the Optical Technology Division of the National Institute of Standards and Technology in Gaithersberg, MD. These calculations indicate that scattered light levels produced from surface dust from mirror coronagraphs will exceed those from lenses by a factor of ~4 (Figure 11). Also, the scattering due to surface roughness is a factor of ~10 larger for a mirror than for a lens with equal roughness. The microroughness curves assume a 1-nm rms finish (integrated from 0.0005 to 100 microns^{-1}) and a power-law slope for the 2-D surface roughness power spectral density of 2.3. Equal surface quality is assumed for the front and rear surfaces of the lens. The dust calculations assume a Class-400 MIL-STD 1246C particle distribution (~0.1% coverage) where all particles above 20 microns have been removed by daily air cleaning. It is assumed that the rear surface of the lens (which resides in a hermetically sealed tube) is cleaned to Class-300 level or better (10^{-4} coverage). The dust is modeled as spherical Mie scatterers with an index of 1.6. The dust scattering calculation uses a "double interaction" model that takes into account the coherent interaction of a particle and its mirror image in the optic. The mirror scattering calculation does not include contributions from coating defects, which may be significant. While the microroughness contribution could be decreased by better optical finishes, the Class-400 dust contamination level is the best level that can be reasonably sustained in COSMO.

Given the scattering advantage of a lens over a mirror, we have chosen to proceed with a refracting design for the COSMO large-aperture coronagraph.

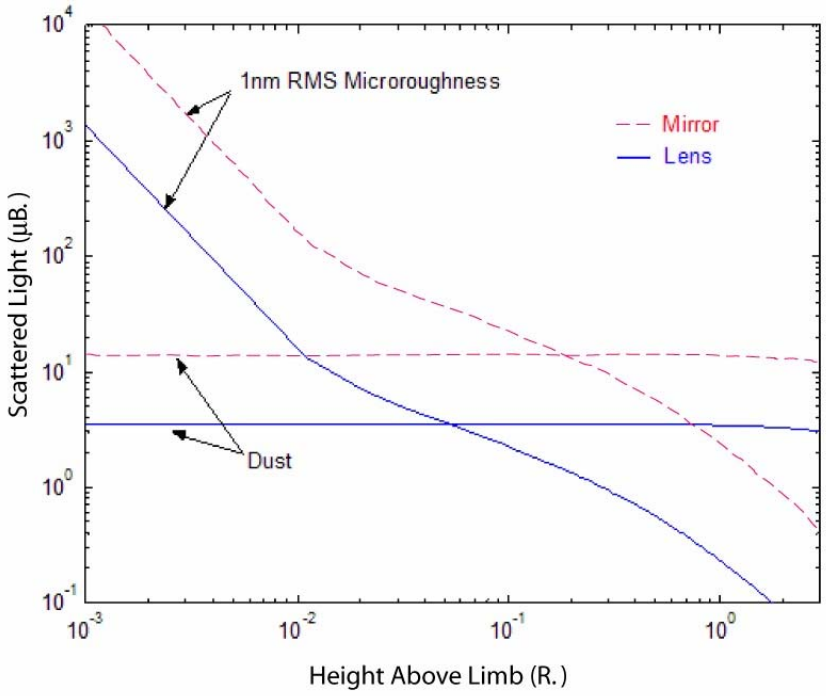

Figure 11 The scattered light level in the coronal FOV due to dust contamination and the quality of the optical finish (microroughness) at 1075 nm shows the advantage of a lens over a mirror and supports a refracting design for the COSMO large-aperture coronagraph. Dust dominates above ~0.1 R_{sun}, while the contribution from microroughness rises steeply at lower heights.

To evaluate the feasibility of constructing a 1.5-m lens, we have conducted a finite element analysis (FEA) of the proposed COSMO lens to determine how its figure is distorted under gravitational and vacuum loadings (Nelson 2006b). The results of this analysis were imported into ZEMAX where the impact on image quality (the point spread function or PSF) could be analyzed. Although gravity can cause up to 5 microns of distortion in the figure, this was found to have a negligible impact on the PSF in either the f/5 or f/7 designs. The FEA analysis also considered stress-induced birefringence, and this was found to be well below acceptable levels.

Given that the largest refracting telescope in existence (Yerkes) has an aperture of 1 m, we understand that the decision to construct a 1.5-m refracting coronagraph will be perceived to entail some risk. However, technology has advanced greatly since the completion of the Yerkes refractor in 1897. Blanks of fused silica of sufficient size and quality are now readily available due, in large part, to developments in support of optical fibers for telecommunications. Fused silica lenses as large as 1.6-m in diameter with extremely high surface quality have already been produced for the National Ignition Facility for laser fusion.

For COSMO, the bulk properties of the fused silica for the lens are also very important and feasible with today's technology. Corning standard-grade 7980 HPFS fused silica is manufactured in single 60-inch-diameter by 8-inch-thick boules as a standard process (large enough for the COSMO objective). It has ~$3 \cdot 10^{-6}$ peak-to-peak index uniformity, less than 1-nm/cm of birefringence, and a stress-optical constant of 3.3 (nm/cm)/(KgN/cm^2). All of these are at least an order of magnitude lower than conventional glasses like BK-7 (used, for example, in the Mk4 coronagraph). The 7980 HPFS fused silica is made in a flame hydrolysis process, which

virtually eliminates striae (layered index variations) as well as inclusions; a single 60-inch boule is expected to have fewer than 20 inclusions in the range of 0.1-0.25 mm. This is about 100 times better than required. Fused silica also has a low level of absorption of solar radiation. This, combined with a higher modulus and lower stress optical constant, make it almost a factor of 10 less sensitive to the deleterious effects of thermal heating. Fused silica has been employed successfully for the primary lens in the ~1-m aperture Swedish Vacuum Telescope and for the vacuum window in the 76-cm Dunn Solar Telescope.

The combination of our engineering studies, recent experience from other researchers, and input from vendors indicates that a 1.5-m coronagraph objective for the COSMO large-aperture coronagraph is well within current technological capabilities. A concept drawing of the COSMO large coronagraph is given in Figure 9.

To meet the science requirements for COSMO, the large-aperture coronagraph should have post-focus instrumentation that includes a narrow-band tunable filter polarimeter and a fiber-fed spectro-polarimeter. Both instruments will obtain precise polarimetry across the emission lines. The instruments are complementary in that they balance differently the trade-off between spectral resolution and FOV. The narrow-band tunable filter polarimeter will observe over the entire FOV with modest spectral resolution as a coronal magnetograph. The fiber-fed spectro-polarimeter will be capable of high spectral resolution line profile observations over a restricted FOV. This combination will support a much wider range of science goals than either instrument could provide individually. The approach of including a filter polarimeter and a spectro-polarimeter was adopted in the Hinode (formerly Solar-B) spacecraft.

An optical design for the large-aperture coronagraph and post-focus instrumentation is shown in Figures 12 and 13. The f/5 fused silica single objective lens forms a color-corrected, 1-degree, full FOV image at the detector plane with 3.5 arcsecond spatial resolution. An occulting disk is located at the prime focus. Optical fibers will divert a portion of the image from a secondary focal plane, while the remainder of the beam will pass through to the dual beam, narrow-band tunable filter polarimeter. The tunable filter polarimeter and the fiber-fed spectro-polarimeter are described below.

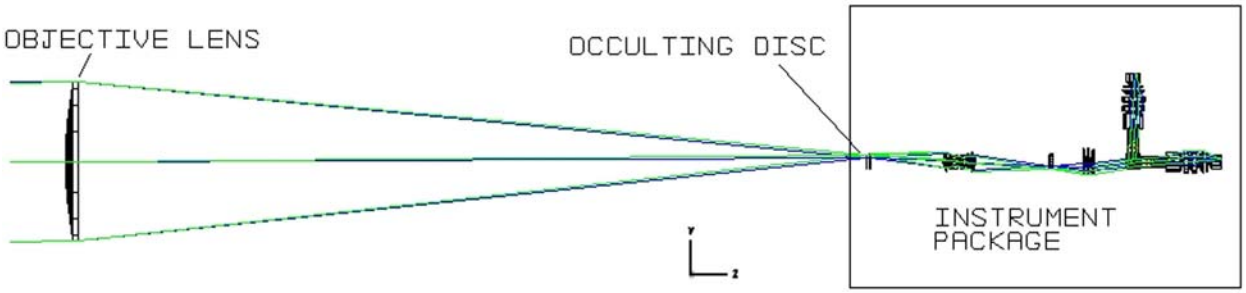

Figure 12 Optical design of the COSMO large-aperture coronagraph. An enlargement of the post-focus instrument section is shown in Figure 13.

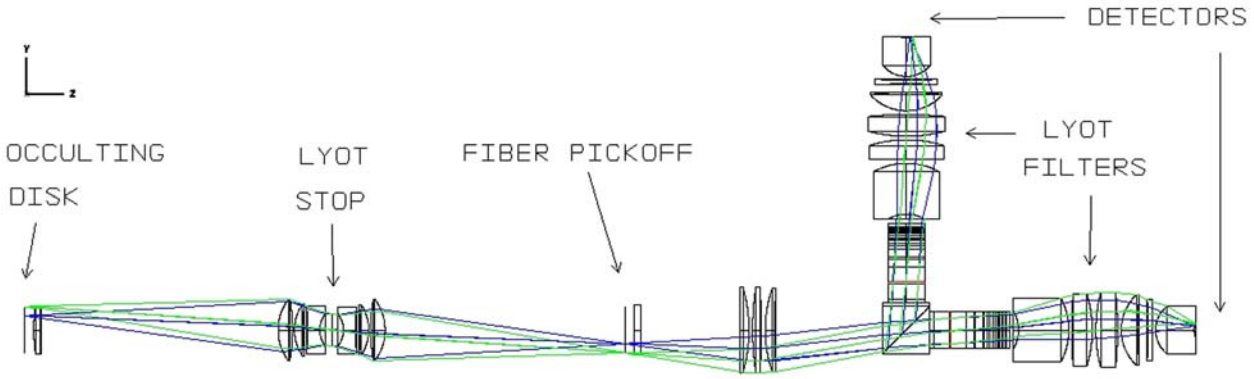

Figure 13 Enlargement of the post-focus instrument section of the COSMO large-aperture coronagraph

3.1.2 COSMO Narrow-band Filter Polarimeter

Observing with a large-aperture telescope over a large FOV is a challenging requirement. The etendue (also called luminosity or throughput) is a property of an optical system defined as the product of the solid angle through each element and the area of the element. To prevent loss of light as it passes through an optical system, the etendue of post-focus instruments must equal or exceed the etendue at the entrance aperture of the telescope. For the COSMO large-aperture coronagraph, the 1.5-m aperture and 1 degree full FOV result in an etendue of 4.23 cm^2 sr. For comparison, the etendue of the 4-m ATST telescope with a 5 arc minute full FOV is 0.21 cm^2 sr. This means that the light-gathering power of the COSMO large-aperture coronagraph will be a factor of 20 times greater than the ATST as long as it is not compromised by the post-focus instrumentation.

The COSMO narrow-band filter polarimeter (NFP) is designed to perform narrow-band coronal filter magnetometry over the entire COSMO field of view. The limiting solid angle that a tunable filter can accept is set by the shift of the passband with incidence angle through the filter. The required passband for the COSMO NFP is set by the width of the FeXIII emission lines (0.14 nm). A survey of available filter technologies determined that the incidence angle sensitivity of simple Michelson and Fabry-Perot interferometers makes them unsuitable for the COSMO NFP, however, a wide-field birefringent filter (Lyot filter) with an aperture of 100 mm constructed with Lithium Niobate crystals can provide a tunable filter with an etendue that exceeds the COSMO requirement by a factor of about 2 (Tomczyk 2006b).

Atmospheric seeing can introduce significant noise into polarization measurements through intensity to polarization crosstalk. To mitigate this source of noise, we have adopted a dual beam design for the COSMO NFP. Polarization selection will be accomplished by the combination of a Ferro-Electric liquid crystal followed by a polarizing beamsplitter. Identical Lyot filters and detectors will be placed in each beam for simultaneous observation of orthogonal polarization states. The baseline detectors are 2048x2048 pixel HgCdTe IR arrays with 1.76 arcsec per pixel. The Lithium Niobate birefringent filters and IR detectors are commercially available.

3.1.3 COSMO Fiber-fed Imaging Spectro-polarimeter

The COSMO Imaging Spectropolarimeter (CIS) is an advanced fiber-optics-based imaging spectropolarimeter that will provide observations over a large FOV with high magnetic field sensitivity and time resolution. Data obtained with this instrument can be used for a wide range of coronal magnetic field research. Its design takes advantage of recent progresses at the University of Hawaii IfA, in large-format IR array detector technology, large-format coherent fiber-optic bundle manufacturing capability, development of low-loss polarization-maintenance multi-mode optical fibers, and multiple-slit spectroscopy techniques.

The CIS will consist of two identical systems. Each system will be equipped with a 128 x 64 format coherent fiber-optic bundle, a large Echelle grating based spectrograph, and a 2048 x 2048 format IR camera. Each coherent fiber-optic bundle will sample the solar corona with 4 arcsec/pixel resolution and cover a 512 x 256 arcsec field. The two fiber-optic imaging arrays will be positioned by a robotic positioning system in the secondary focal plane of the coronagraph for flexible selection of observing targets. Nominally, the two systems patrol the east and west limb active latitudes simultaneously. During active events, the two systems can be combined to observe an expanded field to provide better spatial coverage of the event.

At the exit end of the fiber bundle, the 16,384 fibers of each system will be arranged into 64 parallel linear arrays, each consisting of 512 fibers. Each linear array serves as a "slit" for the spectrograph. Each fiber will be allocated a 4 x 64 pixel x 2 (for two orthogonal polarization states) strips on the 2048 x 2048 IR camera located at the focal plane of the spectrograph. A DWDM-styled filter will limit the spectral window transmitted through the system and remove the overlapping spectra from the parallel slits. This multi-slit spectroscopic technique has been successfully demonstrated by the IfA team (see Lin, Kuhn, and Coulter 2004 and Section 2.4).

The coherent fiber-optic bundle will be constructed with new birefringent multimode optical fibers that are currently being developed by the IfA team. The birefringent optical fiber preserves one of the linear polarization states of the solar radiation as it is transmitted through the optical fiber. Thus, dual-beam polarimetry, in which the orthogonal polarization states (e.g., I+S and I-S) are simultaneously recorded, can be performed through the optical fiber. This configuration minimizes seeing-induced polarization crosstalk, and yields a factor of two increase in overall system efficiency since the two polarization states are recorded simultaneously. The instrument characteristics are summarized in Table 2.

Table 2 CIS Instrument Characteristics Summary

Imaging array format	128 x 64 fibers x 2
Spatial sampling size	4 arcsec per fiber
Field of view	512 x 256 arcsec x 2
Spectral resolution	11.0 pm ($\lambda/\Delta\lambda \sim 10^5$)
Spectral window coverage	0.7 nm
Doppler velocity range	200 km/sec

3.1.4 White-light K-coronagraph

The white-light K-coronagraph is an instrument to measure white light coronal polarization brightness (pB) due to electron scattering of photospheric light by the K-corona. It will reside on the solar pointed spar in the small dome (Figure 17). The design of the K-coronagraph (Elmore 2007a) follows from the desire to provide high cadence observations of CME formation and early acceleration at a cadence and sensitivity greater than those currently available from the Mauna Loa Mk4 K-coronameter. In order to monitor all phases of CME acceleration, the K-coronagraph must provide high signal-to-noise pB measurements over an entire FOV starting only a few hundredths of a solar radius above the limb and extending outward to 2.5 solar radii. Signal-to-noise is limited by photon noise, atmospheric seeing and scintillation by aerosols. The optical design for the K-coronagraph is shown in Figure 14.

Even the lowest scattered light coronagraph designed to observe close to the limb of the Sun has a background light level, which is bright compared to the K-corona. To minimize instrumental scattered light a Lyot coronagraph with a super polished singlet objective lens is used. Sufficient photons must be collected to be able to detect the faint outer corona against the background scatter. A newly designed 2048x2048 pixel deep well area array detector with high frame rate (150 Hz) will be used to rapidly collect these photons over a 5 solar radii full FOV (1.05 to 2.5 R_{sun} above the limb, as measured from sun center) at a spatial resolution of 5 arcsec. The product of the telescope aperture times the wavelength pass band must be wide enough to provide the required photons. A wide pass band is not compatible with occulting close to the limb of the Sun, requiring the use of an objective lens far larger than needed simply to meet spatial resolution requirements. A balance between aperture size and pass band is achieved by using a 20-cm diameter objective and a 25-nm pass band.

Seeing and scintillation can introduce noise into a polarization measurement if the instrument uses a polarimeter to encode the polarization signal into a linear combination of successive camera frames. This cross-talk effect is minimized by operating at a high frame rate and by utilizing dual beam polarimetry. The two beams detect polarization with opposite signs so that their difference detects polarization without variations in intensity masquerading as signal. Aerosols can be strongly polarized and saturate detector pixels. Real-time vision processing of camera data will be used to identify and remove these artifacts from the images.

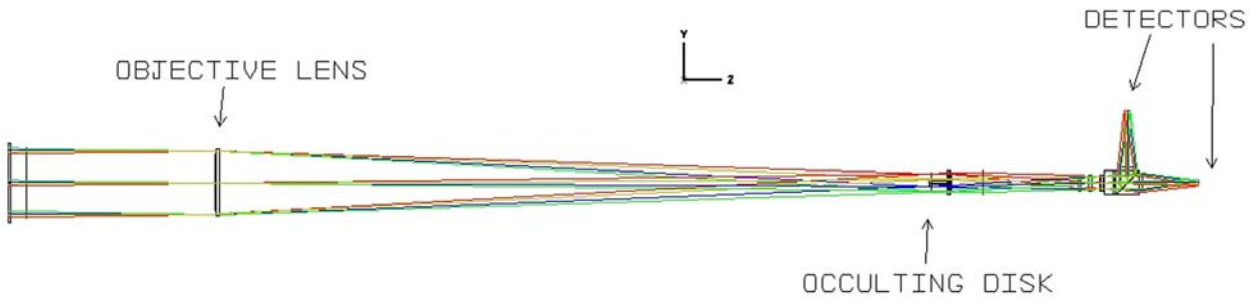

Figure 14 The COSMO white-light K-coronagraph optical layout showing location of detectors

3.1.5 Chromosphere and Prominence Magnetometer

The COSMO chromosphere and prominence magnetometer (ChroMag) is a polarimeter to measure chromosphere and prominence magnetic fields using the chromospheric spectral lines of He I (587.6 and 1083 nm) and Hα (656.3 nm). Measuring prominence magnetic fields embedded within the corona provides a more complete picture of field configurations than could be provided from a coronal or chromospheric magnetometer alone. Simulations of the inversion of magnetic field data in prominences (Casini 2007) indicate that a tunable filter instrument can provide data of sufficient quality to meet the science requirements of COSMO as long as noise can be kept at a level lower than 10^{-3}. The tunable filter also must have a bandwidth of 0.025 nm in the visible region and 0.046 nm in the IR. These requirements are met by the ChroMag design (Elmore 2007b) shown in Figure 15.

The ChroMag is a 20-cm Lyot coronagraph that operates with an occulting disc for prominence measurements above the limb and operates un-occulted for chromosphere and filament measurements on the solar disk. The design maintains an instrumental scattered light level small compared to prominence brightness. Even with this constraint, it is possible to use an air-spaced doublet objective lens allowing for observations over the required large spectral range.

The lens for ChroMag was chosen so that the optical path can have low scattered light and be axially symmetric to minimize telescope polarization. Signal to noise is limited by the total number of photons collected and by atmospheric seeing. High frame rate, 2048x2048 pixel detectors are used in order to perform the polarization measurement rapidly compared to atmospheric seeing and to rapidly collect photons. A dual beam polarimeter is used to minimize seeing-induced cross-talk. In order to make polarimetric measurements spanning the entire solar disc at a high (<1 minute) cadence, ChroMag uses a pair of tunable Lyot filters, one for each of the dual beams. With interchangeable pre-filters to isolate spectral regions around the chromospheric lines of interest, the Lyot filters can be tuned across the spectral lines using liquid crystals on each filter stage. Only about a dozen wavelengths are needed to sample each spectral line and these can be collected in about 15 seconds/line. Scans will be repeated and can be summed to increase signal-to-noise. The ChroMag will have a full FOV of 2.5 solar radii and a spatial resolution of 2.3 arcsec.

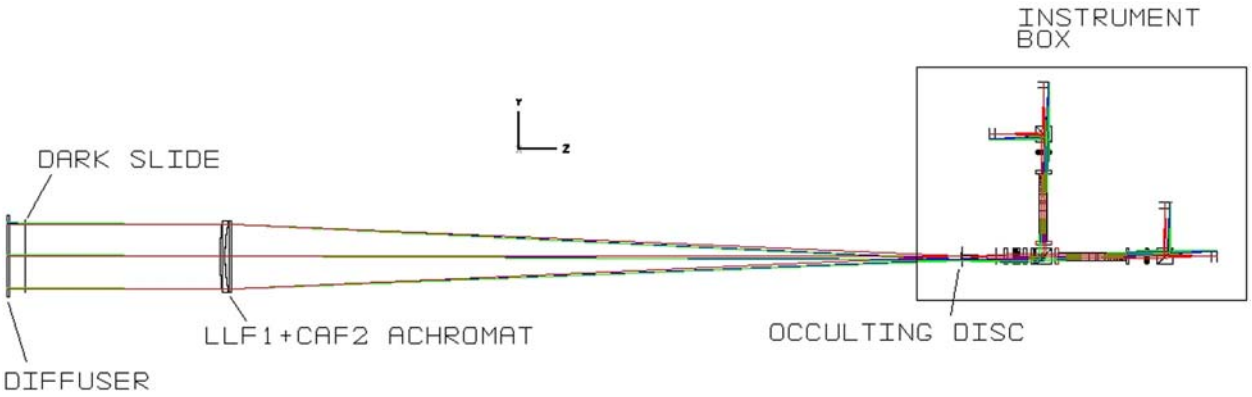

Figure 15 Chromosphere and prominence magnetometer: ChroMag optical layout. The dark slide and diffuser are inserted for calibrations.

3.2 Site Selection and Development Plans

The primary science goal of the COSMO facility is to measure coronal magnetic fields. For the most effective operation, the site should have low sky background, high clear sky fraction, and reasonable spatial resolution (seeing conditions). As discussed in the Section 3.1.1 above, because coronal magnetic field measurements are so sensitive to background light levels, the COSMO facility must be located at a site of extremely low sky background (less than about 5 millionths of the solar disk at 1 μm, on average). Since the synoptic mission of the COSMO facility demands regular observations, another important consideration for site selection is clear skies. The clear time fraction at the COSMO site should exceed 50%. Compared to the requirements for low sky background and high clear sky fraction, the seeing requirement for COSMO is relatively modest. The large-aperture coronagraph and white-light K-coronagraph must form images with a spatial resolution of 5 arcsec, while the chromosphere and prominence magnetometer has a required resolution of 2 arcsec.

These collective requirements place severe constraints on the choice of site for the COSMO facility. The site selection criteria for COSMO are, in order of importance:

(1) Sky brightness—less than ~5 μB_{sun} on average at 1.1 R_{sun} at 1μm
(2) Clear time fraction—greater than 50%
(3) Seeing - better than 2–5 arcsec (for ChroMag/large-aperture coronagraph)

Very few sites are known to have coronal sky conditions that meet these requirements. However, we know that Haleakala and Mauna Loa in Hawaii do meet them. Of the six sites tested for sky brightness by the ATST site survey, Haleakala had the best coronal sky conditions with median sky brightness of 5.8 μB at 1.1 R_{sun} at 1μm. Mauna Loa was not tested for sky brightness in the ATST survey. However, analysis of coronal data collected with the Mk4 coronameter between 2004 and 2006 (Elmore 2007c) estimated sky brightness at Mauna Loa of 0.5μB per airmass for heights between 1.15 and 2.46 R_{sun} . Both Haleakala and Mauna Loa were estimated by the ATST survey to possess 2,800 hours of sunny skies, corresponding to a clear time fraction of about 64%. Haleakala was found in the ATST site survey to possess excellent seeing conditions. Although the seeing at Mauna Loa has not been quantified, the seeing at these two sites in Hawaii is dominated by ground level seeing, which is expected to be comparable for the two sites. The elevations of Haleakala and Mauna Loa are 10,023 ft (3,084 m) and 11,140 ft (3,397 m) respectively.

Since Haleakala and Mauna Loa have observing facilities operated by COSMO member institutions, the University of Hawaii and HAO, these two sites offer great logistical advantages to the project. Given the demonstrated excellent coronal observing conditions of the sites and their logistical advantages, we have decided to forego a worldwide site survey and choose between Haleakala or Mauna Loa for the COSMO facility. This allows us greater resources to carefully evaluate and compare these two sites. Since sky brightness is our most important site selection criterion, we must compare the sky brightness of the two sites in a standard way. To accomplish this, the COSMO project has obtained a Sky Brightness Monitor (SBM) from the ATST project that is identical to the one installed at Haleakala (see Figure 16 left). It has been installed on the spar at Mauna Loa since June 2006 and has been collecting data since that time.

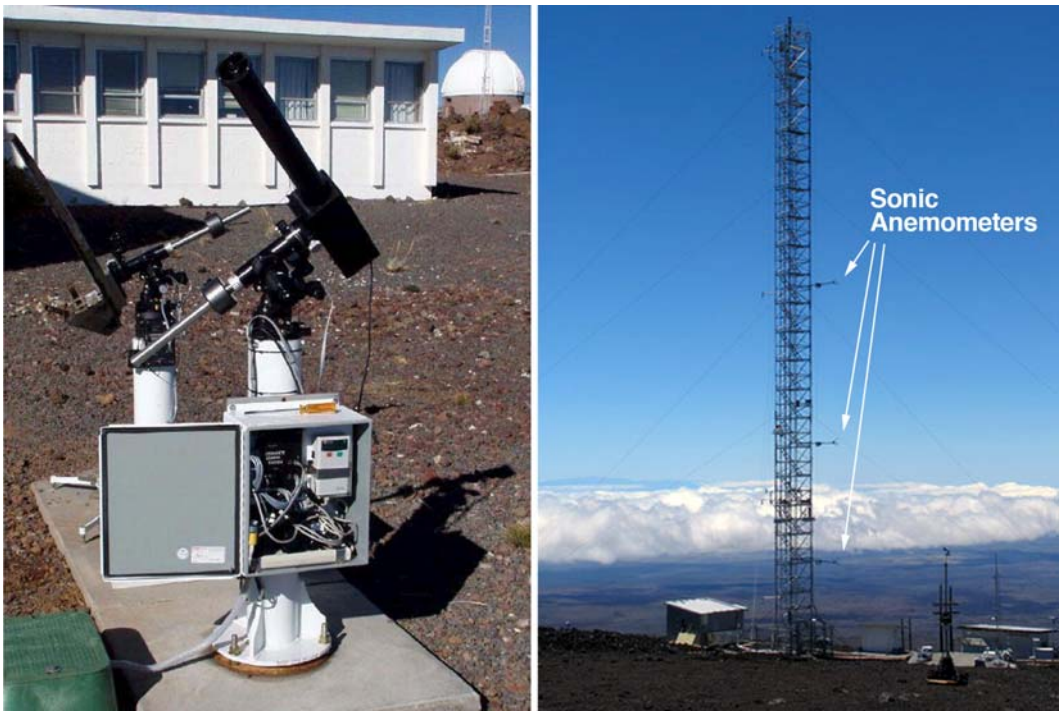

Figure 16 [left] The Sky Brightness Monitor instrument at Haleakala (courtesy of the ATST project). An identical instrument has been installed on the spar at Mauna Loa. [right] Sonic anemometers deployed on the NOAA 40-m tower at the Mauna Loa Observatory evaluate the ground layer seeing. The sonic anemometers were located at 6.0, 13.3, and 23.2m above ground. They were mounted on the east side of the tower because in June and July the prevailing wind is from the northeast.

Seeing during the daytime is generally dominated by thermally induced ground layer seeing. It is therefore important to quantify this source of seeing to determine the best height for the telescope above the ground. The ground layer seeing at Haleakala was measured by the ATST site survey with a scintillometer array, and those measurements were calibrated with anemometer data. The anemometer data provide an unambiguous estimate of the refractive index fluctuations that are responsible for the seeing. In order to quantify the ground layer seeing at Mauna Loa in a consistent way, we conducted a two-month measurement campaign from June 9 to August 8, 2006 with sonic anemometers installed on the NOAA 40-m tower at three heights (6.0, 13.3, 23.2 m; see Figure 16 right). The final choice between Haleakala and Mauna Loa will be made later when the SBM and sonic anemometer data analyses are completed. Preliminary analysis of these data indicates that either site should meet the scientific requirements for the COSMO facility.

The development of any Hawaiian site must be approached with great sensitivity to cultural and environmental concerns. To minimize cultural and environmental impacts, we plan to avoid breaking new ground by building the COSMO facility at locations developed previously for other purposes.

If the Haleakala location is selected, the large-aperture coronagraph dome would be located at the Zodiacal Light telescope site. The K-coronagraph and ChroMag would be deployed onto the existing solar pointed spar at the Mees observatory. Using the Mees spar at Haleakala offers a cost savings for the facility. The drawback of using the Mees spar is that the

ATST is planned to be constructed a short distance away and will shadow the COSMO instruments at Mees for up to two hours daily during a two-month period.

If the Mauna Loa site were selected, the COSMO facility would be located on federally-owned land operated by NOAA. Within the original boundaries set in 1958, the development at that site is exempt from many restrictions that apply to other Hawaiian sites. Nevertheless, COSMO construction would proceed in a way that minimizes environmental impact by locating the large-aperture coronagraph and solar pointed spar in adjacent domes at the location now occupied by the NOAA air sampling tower. The NOAA tower will be moved to the location now occupied by the Mauna Loa Solar Observatory (MLSO). The MLSO is currently in the wind rose of the NOAA air sampling tower, so relocation of that tower would reduce the impact of site activities, including COSMO, on the NOAA air sampling. A rendering of the Mauna Loa configuration of the COSMO facility is shown in Figure 17.

We are discussing deployment of the COSMO facility with representatives from both candidate sites. Cost estimates for the COSMO facility were made assuming the Mauna Loa site.

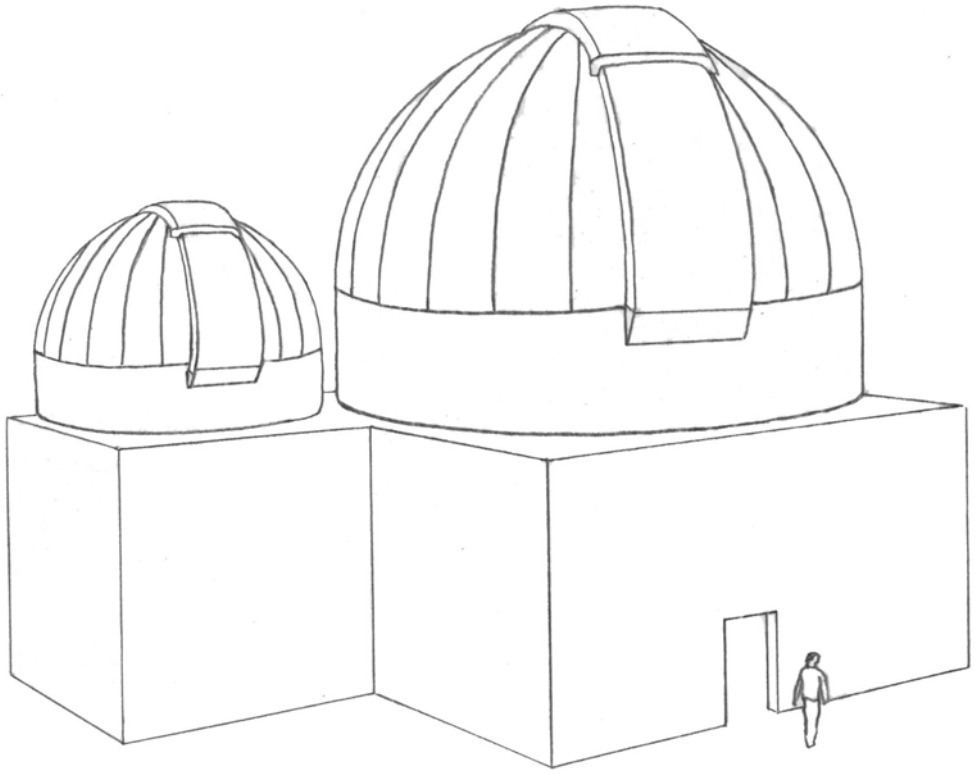

Figure 17 Concept rendering of the COSMO facility appropriate to the Mauna Loa site.

4 DATA OPERATIONS

The primary scientific goal of COSMO is to provide coronal observations to help the scientific community understand the response of the solar atmosphere to changing conditions originating at and below the photosphere. In particular, we hope to understand how solar activity is driven by stresses created by these changes. This goal will be addressed by an observational program that combines elements of a continuous synoptic observing program (about 9 daylight hours every day) with the flexibility to respond to promising new observational ideas through community-sponsored observational campaigns (special limited-duration observing projects). COSMO data operations are divided into two basic parts: observing strategies and data management, both determined by COSMO science requirements. When the facility is completed, operations from MLSO will move to the new COSMO facility.

4.1 Observing Strategies

The synoptic observing program is designed to meet the COSMO science requirements by including the following:

- 10-30-minute time cadence of the coronal, chromospheric, and prominence magnetic fields,
- 15-second time cadence of the polarization brightness of the low corona, and
- 1-minute line emissions of Hα and He I.

Observations will be acquired daily during a nominal 9-hour observing day (~17 UT to 02 UT). Daily, high-time resolution observations are needed to identify and track dynamic events, such as CMEs and prominence eruptions, and to monitor the evolution of the magnetic and density structure of the solar corona.

In addition to the synoptic observing program, observational campaigns sponsored by the scientific community will add flexibility into the COSMO facility operations. These campaigns will be modeled on successful community observational programs such as the NASA SOHO Joint Observing Program (JOP). JOPs increase the scientific return of the COSMO facility by taking advantage of new, promising ideas for using the instruments. Researchers will submit proposals to a COSMO User Advisory Panel comprised of scientists from the solar, heliospheric, and space-weather communities. Approved JOPs may be designed to operate COSMO instruments in ways different from the synoptic program (e.g., higher temporal cadences, off-points, observing other emission lines) or may take advantage of space on the solar spar to incorporate a new instrument that enhances COSMO scientific research.

4.2 Data Management

The COSMO data system infrastructure will utilize various quality controls, pattern recognition software, and solar activity identification routines. The data must be packaged to satisfy scientific interests ranging from the study of dynamic events in near real time to understanding the evolution of the solar corona over time scales of the 11-year solar cycle. To meet this challenge, COSMO will provide all key observations to the user community as a variety of data products: quick-look real-time images, movies, and activity alerts; level 1 data products, activity catalogues, and databases; and level 2 fully processed data products designed

for easy use with other datasets and community models for data mining and reanalysis (Figure 18).

Quick-look data will be supplied in near real time (within minutes of acquisition). Space-weather products such as activity detection and alerts will be given high priority for processing and distribution. Automated schemes will identify dynamic events such as CMEs (e.g. the Cactus software–Royal Observatory of Belgium), optical flares and structures such as solar prominences and filaments. Information from these automated routines will be compiled in online catalogues that are updated regularly.

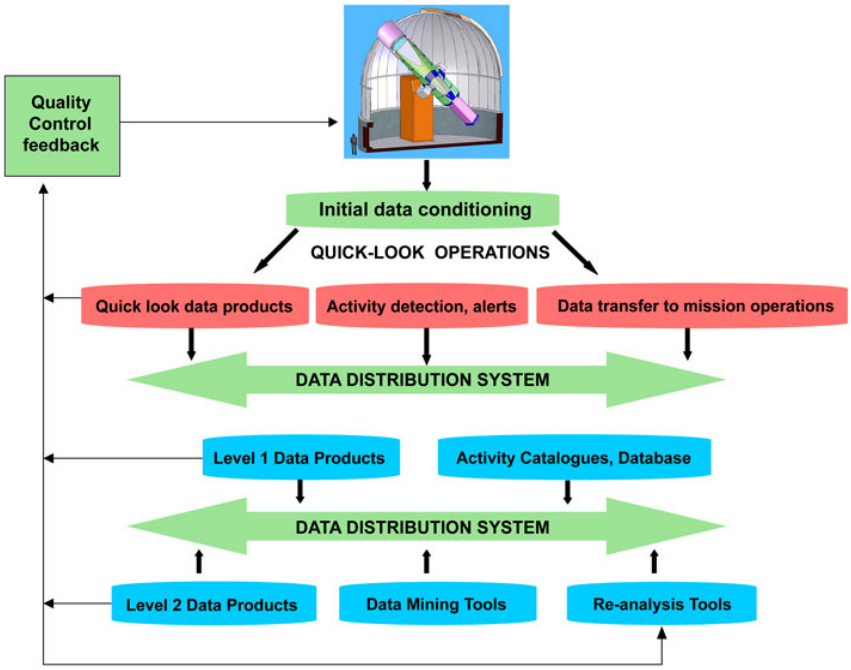

Figure 18 Overview of the COSMO data system architecture. Provides real-time data and alerts as well as higher-level data products to the community. Real-time products for space-weather forecasting will be given high priority.

The key magnetic field observations will be provided in a variety of ways. Level 1 data will include fully-processed Stokes profiles from the corona and chromosphere. Level 2 data will include magnetic field maps and images of the corona and chromosphere, including prominences and filaments from the He I 587.6- and 1083-nm lines. Maps include the strength, inclination, and azimuth of the magnetic field. Images of the low corona from Fe XIII 1074.7- and 1079.8-nm at line center include the linear polarization; the direction of the magnetic field in the POS; the LOS magnetic field strength; the LOS plasma velocity; and images of the coronal density from the Fe XIII line ratios (see Figure 6). The white-light K-coronagraph will provide 15-second time cadence images and movies of the low corona for detecting solar activity such as CMEs, prominence eruptions, and associated waves. Images will be provided in FITS format, which is widely used by the solar and space-weather communities, and in a quick-look, easy-to-use format such as jpeg. These data products will be produced by calibration routines devised at HAO/NCAR. The COSMO User Advisory Panel and COSMO investigators will identify other useful data products that are consistent with available data management resources.

In addition to the data products listed above, the COSMO team will provide additional products designed for easy integration with other solar observations and community models. The goal is to maximize the use of the coronal magnetic field observations, particularly by scientists who are less familiar with the use of spectro-polarimeteric data. These higher-level products will be designed by the COSMO team institutions, led by the University of Michigan, in close consultation with the COSMO User Advisory Panel. The panel will help to identify the most appropriate scientific models, such as those provided by the Community Coordinated Modeling Center (CCMC), and methods for integrating COSMO data with new observations that take advantage of the most recent scientific findings. The data management system will be highly distributed, reliable, and designed to scale upward to take advantage of technological innovations and to meet future scientific goals.

The vast majority of data are generated from the magnetic field observations since the detectors are large and all four Stokes profiles are recorded. Both the large-aperture coronagraph and the ChroMag will have 2K x 2K detectors to record each of the four Stokes profiles (*I,Q,U,V*) at 2 bytes/pixel. Together, the Stokes profiles in the two Fe XIII lines from the large-aperture coronagraph and the He I lines from ChroMag generate 68 MB of uncompressed data every second (see Table 3) at a cadence of 1 minute time cadences to study solar activity and waves. Significantly lower time cadences (30 minutes) are needed to study the quiet corona. We estimate that ChroMag will observe, on average, for 7 hours per day, 330 days per year and the coronal telescopes will be able to observe, on average, for 5 hours per day, 300 days per year, as shown in Table 3. Observations of the chromosphere are much less sensitive to sky conditions, and it is possible to acquire chromospheric images during periods of light cloud cover that otherwise obscure the solar corona. These estimates are based on the actual average amount of observations acquired of the chromosphere and corona at Mauna Loa over the past 4 years, based on the three-person observing schedule to be used by COSMO. Based on these averages, we estimate that COSMO will acquire 1.6 terabytes (TB = 10^{12} bytes) of raw, uncompressed data per day.

Data storage at the observing site should have the capacity to store between two to four weeks of observations to handle unforeseen circumstances such as data transmission and systems failures. This requires a storage system capacity of 22 to 44 TB at the observing site. Data archive systems with these capacities are readily available today at costs of about $100K. Data storage costs are expected to drop dramatically over the next five years, based on industry commitments.

COSMO observations will be stored in “streaming” mode that allows for efficient and lossless compression (factors of 4 to 10) and transmission of data from the observing site to the main computing facility. A modest data compression factor of 2 would require data transfer rates of 32 MB/sec from the observing site to the NCAR data facility for a period of 5 to 7 hours per day, or ~8 MB/sec over a 24-hour period. K-band (10.9 GHz to 36 GHz) transmission rates between ground and satellites can currently handle these data rates. The Tracking and Data Relay Satellite System (TDRSS) currently provides 150 MB/sec to White Sands and up to 50 Mbytes/second to the South Pole research stations. Faster and more widely available K-band services are currently under development. Frameworks such as the Open-Source Project for Network Data Access Protocol that optimize data connections between local and remote locations will be adopted for COSMO.

Table 3 COSMO Data Storage and Processing Requirements

COSMO Raw Data (uncompressed)

	Number of Detectors	Horiz Pixels	Vert Pixels	Bytes/pixel	Wavelength Samples	Number of Stokes	Cadence (s)	Data Rate (MB/s)	Hours/day	Days/year	Data/Year (TB)	
ChroMag	2	2048	2048	2	12	4	15	53.69	7	330	446.46	
Filtergraph	2	2048	2048	2	5	4	30	11.18	5	300	60.40	
Spectropolarimeter	2	2048	2048	2	1	4	30	2.24	5	300	12.08	
K-coronagraph	2	1024	1024	2	1	3	15	0.84	5	300	4.53	
										Raw Data/Year	523.47	(TB)
										Continuous Data Transfer Rate	16.60	(MB/s)
										Total Samples/Year	261.73	
										Operations/sample for Level 1 Processing	100	
										Computation Rate for Level 1 Processing	0.83	(GHz)

COSMO Level 1 Data Products (calibrated, flat fielded)

	Number of Data products	Horiz Pixels	Vert Pixels	Bytes/pixel	Number of Lines	Number of Stokes	Cadence (s)	Data Rate (MB/s)	Hours/day	Days/year	Data/Year (TB)	
ChroMag	12	2048	2048	4	4	4	300	10.74	7	330	89.29	
Filtergraph	1	2048	2048	4	2	4	300	0.45	5	300	2.42	
Spectropolarimeter	1	2048	2048	4	2	4	300	0.45	5	300	2.42	
K-coronagraph	2	1024	1024	4	1	1	15	0.56	5	300	3.02	
										Level 1 Data/Year	97.14	(TB)
										Total Samples/Year	24.29	
										Operations/sample for Level 2 Processing	10000	
										Computation Rate for Level 2 Processing	7.70	(GHz)

COSMO Level 2 Data Products (images of magnetic field parameters, synoptic maps)

	Number of Data products	Horiz Pixels	Vert Pixels	Bytes/pixel	Number of Lines	Number of Stokes	Cadence (s)	Data Rate (MB/s)	Hours/day	Days/year	Data/Year (TB)	
ChroMag	12	2048	2048	4	4	4	300	10.74	7	330	89.29	
Filtergraph	7	2048	2048	4	2	1	300	0.78	5	300	4.23	
Spectropolarimeter	7	128	128	4	2	1	300	0.00	5	300	0.02	
										Level 2 Data/Year	93.54	(TB)
										Total Yearly Data Storage Requirement	714.15	(TB)
										Total Yearly Data Processing Requirement	8.53	(GHz)

The COSMO data archive will be multi-tiered, with quick-look and higher-level data products stored on a high-speed delivery system at HAO. COSMO will take advantage of technologies being developed by virtual observatories, including the NSF-sponsored Virtual Solar-Terrestrial Observatory (VSTO) at NCAR and the Virtual Solar Observatory (VSO) at NASA/Goddard Space Flight Center. The key to efficient data retrieval is to store appropriate metadata into the database and to devise thorough, flexible, and reliable responses to data queries. The performance of these queries will be significantly improved by the introduction of oncology-based schemes implemented through the VSTO.

COSMO data storage and processing requirements are significant, but less demanding than many of today's large observational and modeling projects in the weather, climate, and astronomical communities. Increases in the computing performance and archive capacities are being driven by projects like the Coordinated Observation and Prediction of the Earth System (COPES) and the Large Synoptic Survey Telescope (LSST). The scientific requirements of these diverse groups call for facilities to handle sustained data rates of hundreds of MB/second from remote observing sites and for storage capacities in the exabyte (10^{18} bytes) range. The total amount of COSMO data (raw and processed), as shown in Table 3, is expected to be 714 TB per year. Higher-level data products will require 190 TB of storage per year (see Table 3). Data archive systems with petabyte (PB = 10^{15} bytes) capacity are expected to cost less than $50K in the next five years (see www.lssto.org/Project/docs/lsst_data_man_prospects.pdf) providing rapid and efficient delivery to the user community. All raw and processed data will be stored at the new NSF-sponsored NCAR data center that is expected to be completed in 2011. The new data center will provide up to 50 PB of storage per year, which is sufficient to accommodate COSMO requirements of 0.7 PB per year. Over the next five years, data storage tapes with capacities of 8 TB are expected to be available at a cost of $100 to $150 per tape on the NCAR mass storage system. Based on these industry commitments, the annual tape costs for storing COSMO data are expected to be under $15K per year.

These estimated storage requirements assume that all data will be permanently archived. In fact, observations acquired under questionable weather conditions, introduce large noise into the observations. These data can be averaged and stored at lower time cadences (5 minutes). Based on the high-quality observing conditions at the Hawaii sites, we anticipate that most data (>75%) will be of sufficient quality to be permanently stored at full resolution.

In addition to data storage requirements, we examine the computational needs of COSMO. The creation of chromospheric magnetic maps from Stokes parameters is the most computationally demanding of all the data processing tasks. We estimate that computer operations for processing raw data and creating higher-level data products will require up to 9 GHz per year of computer processing, the most demanding of which can be performed on the high-speed NCAR computing machines. The new NSF-sponsored NCAR data center scheduled for completion in 2011 will provide petaflop (10^{15} operations/second) computing capacity from 100,000 processors. The raw data processing and less computationally-demanding coronal magnetic maps can be performed on multi-processor LINUX boxes at HAO for under $100K. The creation of data products for comparison with and assimilation into models will be performed at the University of Michigan.

HAO/NCAR has recently hired one full-time, high-level programmer to begin the design of the next-generation data pipeline that can be used by COSMO. Two FTEs at HAO/NCAR are currently working with Mauna Loa data and will assist in the COSMO data design. We anticipate

an additional FTE will be needed to fully design and execute the software needed to process COSMO observations. COSMO will incorporate tools currently under development through an NCAR-sponsored initiative to create magnetic maps and images from Stokes profiles acquired in the photosphere and chromosphere. Once COSMO is complete, the three FTEs currently at HAO/NCAR will transition to COSMO data processing.

COSMO data will be available over the Internet from the COSMO Web site (http://www.cosmo.ucar.edu), which will replace and incorporate the current MLSO data archive (http://mlso.hao.ucar.edu). HAO currently provides all MLSO coronal and chromospheric data (2-3 terabytes) recorded from 1980 to present. These data will become part of the COSMO archive, providing observations to the community over multiple solar cycles.

4.2.1 Quality Control

HAO/NCAR staff will be responsible for quality control feedback to ensure the proper operation of the instruments and the integrity of the observations. Routine processing and validation checks will be performed in near real time by automated routines and by HAO staff at the observing site and at NCAR to guarantee proper operation and function of the telescopes and the integrity of the data. The University of Michigan will be responsible for creating high-level data products for integration with community models, in close consultation with the COSMO User Advisory Panel. The three Principal Investigators will work closely with the User Advisory Panel to make sure the COSMO observations continue to offer the most significant and highest quality data to the community.

4.2.2 Transition of Operations

The new COSMO facility is expected to take five years to complete. During that period, observations of the corona and chromosphere will continue at Mauna Loa without significant data gaps. A smooth transfer of operations to the new facility will be planned with minimal downtime. HAO/NCAR and University of Hawaii staff will supervise the construction and transfer phases at the new Hawaii site. We anticipate minimal downtime while the current instrumentation is moved.

5 DATA ANALYSIS

We will utilize a number of tools to compile the most complete set of information from the COSMO instruments. These tools are divided into three broad topics:

(1) HAO inversion methods that are used to convert Stokes vectors into field parameters
(2) Coronal seismology, which is the study of coronal waves that provides powerful diagnostic tools for probing plasma and magnetic field conditions
(3) Models to resolve the optically thin corona integrated along the observer's LOS

5.1 HAO Inversion Codes

The spectro-polarimetric data acquired by some of the instruments described in this prospectus carry the information on the magnetic field and thermo-dynamic state of the emitting plasma. The process of extracting this information from the observed data can generally be termed "data inversion." However, different strategies to accomplish this task can be devised depending on the characteristics of the dataset.

As Section 5.3 shows, the interpretation of coronal data is better achieved by comparing the observed polarization with the results of forward radiation modeling, operated on a careful selection of theoretical models of coronal magnetism. This is because the observed radiation typically samples a very large volume of the optically thin coronal plasma. The inversion problem is intrinsically under-constrained when a virtually infinite set of magnetic configurations is mapped into the four independent Stokes parameters needed to describe the observed polarized radiation (Judge 2007).

When, instead, the observed radiation is sampling only a relatively small and well-localized plasma volume in the corona, then a one-to-one correspondence between the (average) magnetic configuration in the plasma and the observed radiation can be assumed. Under these circumstances, spectro-polarimetric data inversion becomes a tractable problem. This is often the case for the observation of prominences and filaments. For the forbidden emission lines observed in the corona, this inversion is based on the Zeeman+scattering polarization formalism discussed in Section 2.2. In the case of the spectral lines of permitted transitions in prominences, one has to rely on the significantly more complex modeling of the Hanle effect (see Section 2.2).

Over the past five years, HAO has led the development of inversion tools for the resonance scattering polarization produced in prominences and filaments. Because the atomic physics involved in resonance scattering is considerably more complicated than in the formation of photospheric lines, the usual nonlinear least-squares inversion approach cannot offer any efficient solution. The strategy that we have followed at HAO is similar to direct forward modeling; the output radiation from many different possible magnetic configurations and thermo-dynamic conditions of the plasma are compared with the observations searching for the best match. In order to make this comparison efficient, a database of the output (Stokes profiles) of these many models is created as a look-up table for the observations. Because of the high dimensionality of the physical problem (i.e., many physical parameters are involved in the determination of the output radiation), this type of database can become extremely large if the full spectro-polarimetric information (Stokes vector) gets recorded. For this reason, a compression scheme must be devised, as discussed below.

Extensive experience in spectro-polarimetric inversion, accumulated over the past ten years, has led to the conclusion that a high level of redundancy is contained in a typical spectral Stokes profile. A carefully selected subset of data points should be sufficient to retrieve the full magnetic information practically without loss. Repeated observations of different solar structures have also confirmed that Stokes profiles originating from the same type of structure show many similarities.

The Principal Component Analysis (PCA) of such Stokes profiles is able to pick out the fundamental similarities between the observed profiles and those contained in the database (containing a few hundred thousand samples), which then can be assumed to be universally present in all datasets produced under the same physical conditions. These universal features form a "basis of eigenprofiles," which does not need to be recorded for every single model in the database. Instead, the database can simply contain the eigencoefficients that are derived from projecting the Stokes profiles of a given model in the database onto the basis of eigenprofiles. The comparison between the observations and the models in the database is then performed by comparing the corresponding eigencoefficients. The best match is determined by minimizing the Euclidean distance between models and observations in the space of the eigencoefficients, and therefore it is completely analogous to a least-square fitting of the observed profiles. Since searching through a database and calculating a Euclidean norm are intrinsically fast operations, the PCA inversion of spectro-polarimetric data is much more efficient than nonlinear least-squares inversion; a complete magnetic map of a prominence can be produced in a matter of minutes. All the complexity of the atomic physics and of the various scattering geometries involved in the forward modeling of prominence and filament data is dealt with upfront during the creation of the model database and does not interfere with the search algorithm actually performing the inversion. The main issues associated with PCA inversion are the discreteness of the model database, which contributes to the inversion error, and the fast-growing rate of the database size in the pursuit of its completeness ("filling the gaps"). Due to the complexity of the polarized radiative transfer in prominences and filaments, compared to the relative simplicity of our current understanding of their structures, typically one hits the error threshold determined by the inadequacy of the model much before the size of the database becomes unmanageable.

5.2 Coronal Seismology

The detection of Alfvén waves with the CoMP instrument, discussed in Section 2.4, paves the way for the use of coronal seismology to provide additional important information on coronal plasma and magnetic fields and also to provide information on physical processes responsible for coronal heating. The theory of MHD waves and oscillations in the corona has been well developed over the past few decades despite the scarcity of observations. Over the past decade, observations of the corona in extreme ultraviolet wavelengths from SOHO and TRACE have detected oscillating loops and propagating waves but not Alfvén waves. Alfvén waves propagate along magnetic field lines and are essentially non-compressive making them difficult to detect in intensity but visible in Doppler shifts. These Doppler shifts are detectable in observations provided by CoMP, though with limited signal and resolution. Observations provided by COSMO offer significant improvements in the detection of Alfvén and other waves in the corona. The properties of Alfvén, as well as magnetoacoustic, waves depend strongly on the direction of wave propagation relative to the magnetic field, making them sensitive to the plasma structure. Variations in the coronal field and plasma can modify the wave properties and

may result in coupling between different wave types. Therefore, in addition to using Alfvén waves to probe plasma and magnetic field conditions in the corona, the study of coronal wave propagation with COSMO will likely lead to new discoveries of a more fundamental nature regarding coronal heating, the acceleration of the solar wind and processes such as phase mixing, resonant absorption, wave excitation, and mode conversion.

5.3 Models

To prepare for the exploitation of COSMO observations, we have started developing tools and techniques for comparing forward models of coronal magnetic fields with observations from CoMP and Solar-C, as well as with anticipated observations (Judge, Low and Casini 2006). Figure 19 shows a simulation of an axisymmetric equatorial current sheet embedded in the Sun's corona as it would be observed by the Fe XIII emission line at 1074.7 nm. The model utilized for the computation of the polarized scattered radiation is based on the formalism of the Zeeman+scattering polarization described in Section 2.2. The current sheet is derived from the analytical model of Low, Fong, and Fan (2003). The plasma is optically thin and has been integrated along the LOS. The plasma is hydrostatically distributed at 1.6 MK, and spherically symmetric. The strength of the linear and circular polarization is shown for two cases; in Figure 19, the top two panels are for a current sheet with sufficient magnetic free energy to launch a CME, while the bottom two panels show the case of a weaker current sheet with insufficient energy for CME launch. Both cases have an identical value of the radial component of the magnetic field at the solar surface. However, the coronal polarization signatures are extremely different for the two cases. This example illustrates the sensitivity of measurements of the polarization of coronal emission lines to the degree of magnetic free energy. These differences in linear and circular polarization signals will be measurable by COSMO over scientifically interesting spatial and temporal scales.

In addition to forward modeling, a number of other methods have been recently developed to determine the three-dimensional structure of the corona along the optically thin LOS. These include dynamic stereoscopy and inversion methods (Aschwanden, et al. 1999; Hayes, Vourlidas and Howard 2001). Stereoscopy uses solar rotation to determine the three-dimensional structure of the corona, but is limited to large-scale structures that vary slowly in time (days). These theoretical preparations will lay the groundwork for the facility proposed here and allow the community to fully and rapidly exploit the potential of these new observations.

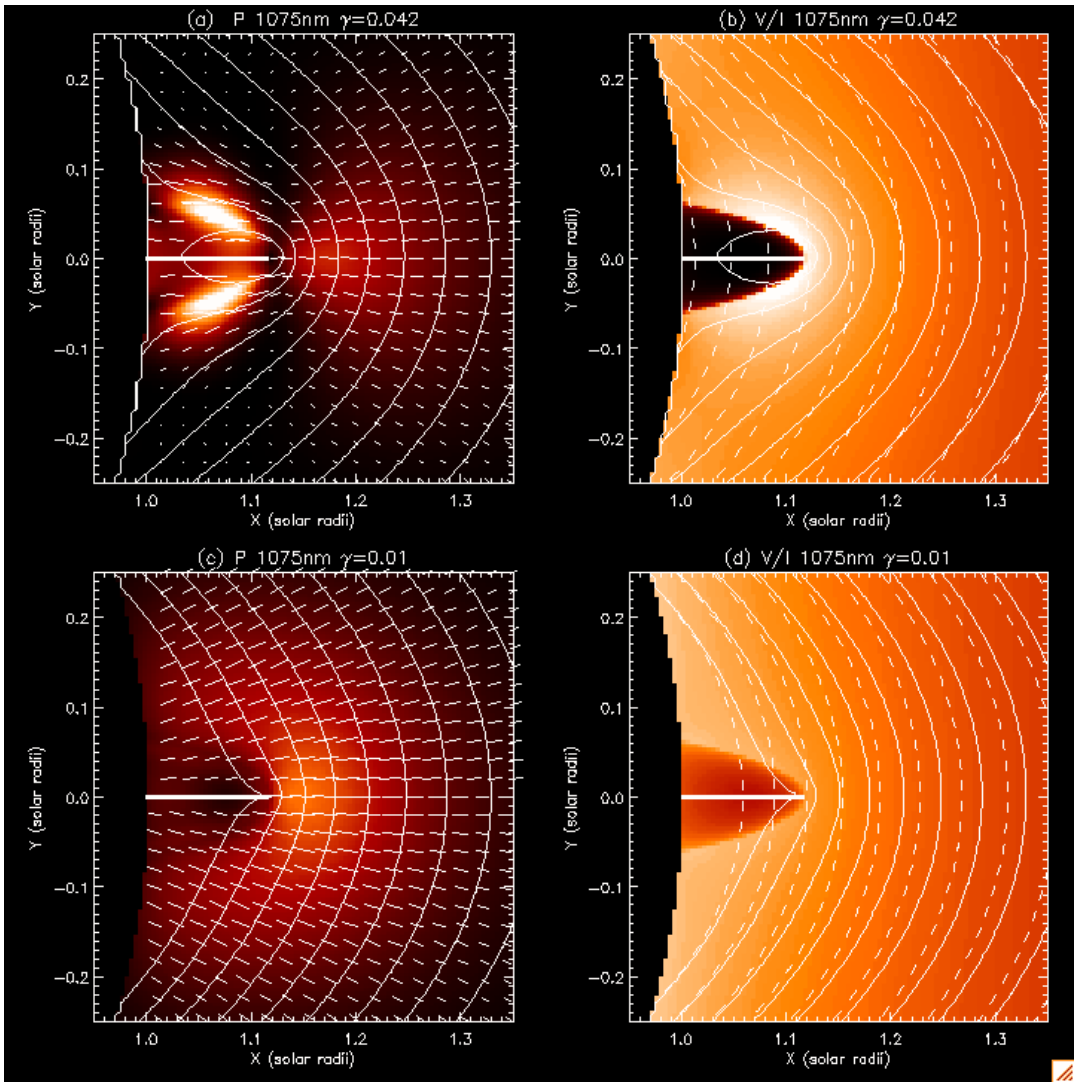

Figure 19 Synthetic images showing sensitivity of Stokes parameters in the Fe XIII line at 1074.7 nm to the presence and strength of an axisymmetric equatorial current sheet in the Sun's corona. These images have 4x4 arcsec resolution. Panel (a): Magnitude (image density from 0 to 5 erg cm^{-2} s^{-1} sr^{-1}) and magnitude and direction of linear polarization P (short lines) computed for a relatively strong current sheet with sufficient magnetic free energy to launch a CME. Solid lines are magnetic field lines. Panel (b) Stokes *V/I* (relative circular polarization between $\pm 10^{-3}$) for the same case as seen from the Earth with the Sun's magnetic S. pole inclined toward us by 7 degrees. Dashed lines show a global dipolar magnetic field which has the same radial magnetic field at the surface as the current carrying case. Panels (c) and (d) show the same calculations for a weaker current sheet with insufficient energy for CME launch. Note the very different polarization signatures of the two cases.

6 EDUCATION AND PUBLIC OUTREACH

Due to its scientific relevance and its expected far-reaching impact, COSMO will advance a new paradigm of community involvement and innovation. The targeted community is focused on, but not limited to, US universities pursuing solar and heliospheric research. As stated by the most recent National Research Council decadal review of research strategy in solar and space physics (Lanzerotti 2003), this community has declined in numbers over several years. It has been strengthened with an NSF program that supported new hires in solar and heliospheric physics at US universities. However, the review identified a perceived lack of involvement by the extended university community in solar observational methods and primary data analysis, which affects the nation's know-how in these important fields. COSMO will address this weakness through a five-pronged strategy:

6.1 Community Involvement Strategy

Open data policy
COSMO will adopt an open data policy. The data dissemination process will follow strategies developed for the Mauna Loa facility, which uses modern web-based technologies that provide complete online Internet access to all data acquired since 1980. Mauna Loa data are currently used by hundreds of scientists and students from ~150 institutions worldwide (See Appendix 9.2). HAO/NCAR currently operates and maintains the Mauna Loa Observatory (since 1965) with three full-time observers at Mauna Loa and three full-time staff at HAO/NCAR to process, calibrate, archive, and distribute all observations in near real time. HAO/NCAR will continue to provide this level of support to the COSMO observatory. Similar programs were also developed by the University of Michigan for space-borne instrumentation, and this experience is also available to the COSMO team. The community participates in the COSMO program through the User Advisory Panel (UAP), which will help create data products, instrument upgrades, and observation campaign goals.

Students involved in all phases of the COSMO project
COSMO creates opportunities for students and university groups to participate in all phases of the project, providing direct access for students and their advisors in the development of breakthrough instrumentation, data analysis, and data product design. Undergraduate and graduate students will be involved through the participating universities and through dedicated HAO/NCAR summer and visitor programs. A specific opportunity will be made available for COSMO PhD fellowships, selected through a national competition that will be run through the NSF or through the UAP. These fellowships will involve hands-on experiences with COSMO that can either focus on technology development or data analysis. Existing community outreach programs successfully implemented at HAO/NCAR, such as the faculty visiting program and others will also strengthen student involvement with COSMO.

COSMO facility in campaign mode
The potential of the COSMO facility cannot be fully exploited without direct community involvement through targeted observational campaigns. Through proposed campaigns, certain science topics will be pursued, which require coordination between the COSMO instruments or between COSMO and other observational tools on the ground or in space. The COSMO

community involvement strategy draws on experiences of the SOHO joint observation program, which pioneered campaign events for enhanced science impacts of SOHO instruments. COSMO campaigns will be selected by the UAP. Care will be taken that these campaigns allow COSMO to pursue its synoptic mission.

COSMO facility as a test bed for breakthrough technology development
Operating COSMO as a test bed addresses an important need in solar and heliospheric physics by providing a place where new technologies developed in the community can be adequately tested. The COSMO facility will encourage these interactions by providing easy access to test technology development efforts typically funded through independent investigations. The multi-instrument nature of the COSMO facility enables this interaction without jeopardizing the primary science. This success of test bed operations will be ensured by a rigorous selection process directed by the UAP.

COSMO education and outreach collaborations
The COSMO facility will collaborate with NCAR's Windows to the Universe education and outreach project (Website and professional development program), which brings the Earth and space sciences to more than 16 million learners and educators each year. This international project is presented in English and Spanish. Information, images, and visualizations resulting from COSMO research will be integrated into the extensive content infrastructure of the Website, and researchers utilizing COSMO will have the opportunity to post "Postcards from the Field," using NCAR's Web-based template format, to highlight progress in their research to the public, students, and teachers. We will also highlight COSMO research in our professional development activities through Windows to the Universe and the NCAR Public Visitors Program, which includes both classroom and exhibit components. We will update our existing exhibit for the public in the NCAR Mesa Laboratory on Sun-Earth system processes to include a highlight on the COSMO facility. COSMO science will impact the next generation of scientists and engineers.

6.2 Relevance to NSF and Other Agency Programs

Observations provided by COSMO will directly address many of the outstanding science challenges identified by national programs including the NSF National Space Weather Program, the NSF-sponsored Solar Heliospheric and Interplanetary Environment (SHINE), and by the NASA Living With a Star program. Furthermore, it provides essential, and otherwise unavailable, observations of the coronal magnetic field needed to solve the most important questions of the solar and heliospheric community as identified in the National Research Council decadal review of research strategy in solar and space physics (Lanzerotti 2003). In addition, COSMO strengthens solar and heliospheric research at universities by offering unique opportunities for students and faculty to participate in development of state-of-the-art instrumentation and methods to combine new observations with community models.

7 MANAGEMENT AND BUDGET

The management plan for the COSMO project is based on the partners' experience designing, constructing, and operating synoptic and campaign-mode solar observational facilities and instruments over the past three decades. It combines centralized management of the facility, technical development, budget, and quality assurance, with science oversight and direction from the broader user community during both the implementation phase and the operational phase. The result will be an observatory facility that makes breakthrough technology available to the widest relevant solar research community through an open data policy.

7.1 Organizational Structure

7.1.1 Facility Governance

COSMO is envisioned as a Mid-Size-Infrastructure community facility sponsored by the National Science Foundation (NSF). The scientific goals, fundamental policies, observational requirements, and general modes of operation will be determined by NSF in consultation with review and advisory panels of its choosing. Functional and financial management of the facility will be conducted through delegation to National Center for Atmospheric Research (NCAR) and performed by its High Altitude Observatory (HAO), which is a division of the NCAR Earth and Sun Systems Laboratory (ESSL). A team of three Principal Investigators from the three primary participating institutions, HAO/NCAR, the University of Michigan, and the University of Hawaii, will direct the Design and Development phase of the project under the guidance of the solar physics community as represented by a Science Advisory Panel (SAP). During the Operational phase, this function will cede to a User Advisory Panel (UAP). The Project Scientist, Steven Tomczyk, will have overall responsibility for design and development activities at HAO/NCAR, with detailed management of the project under the direction of an experienced engineering project manager (Figure 20).

7.1.2 Project Oversight Team

The COSMO project is directed by three Principal Investigators who will provide overall guidance, decide significant technical issues, respond to the requirements of the SAP, and report to NSF management.

- Steven Tomczyk of HAO/NCAR will manage financial and administrative aspects of the facility. He will direct the COSMO engineering team at HAO through the Project Manager and utilize the engineering and administrative resources of HAO/NCAR to build and operate the facility.

- Thomas Zurbuchen, University of Michigan, chairs the SAP. He will also manage the specification and development of data analysis methods and data products to be used for model comparisons.

- Haosheng Lin, University of Hawaii, will design and fabricate the fiber-fed spectro-polarimeter instrument. He will also participate in data analysis activities.

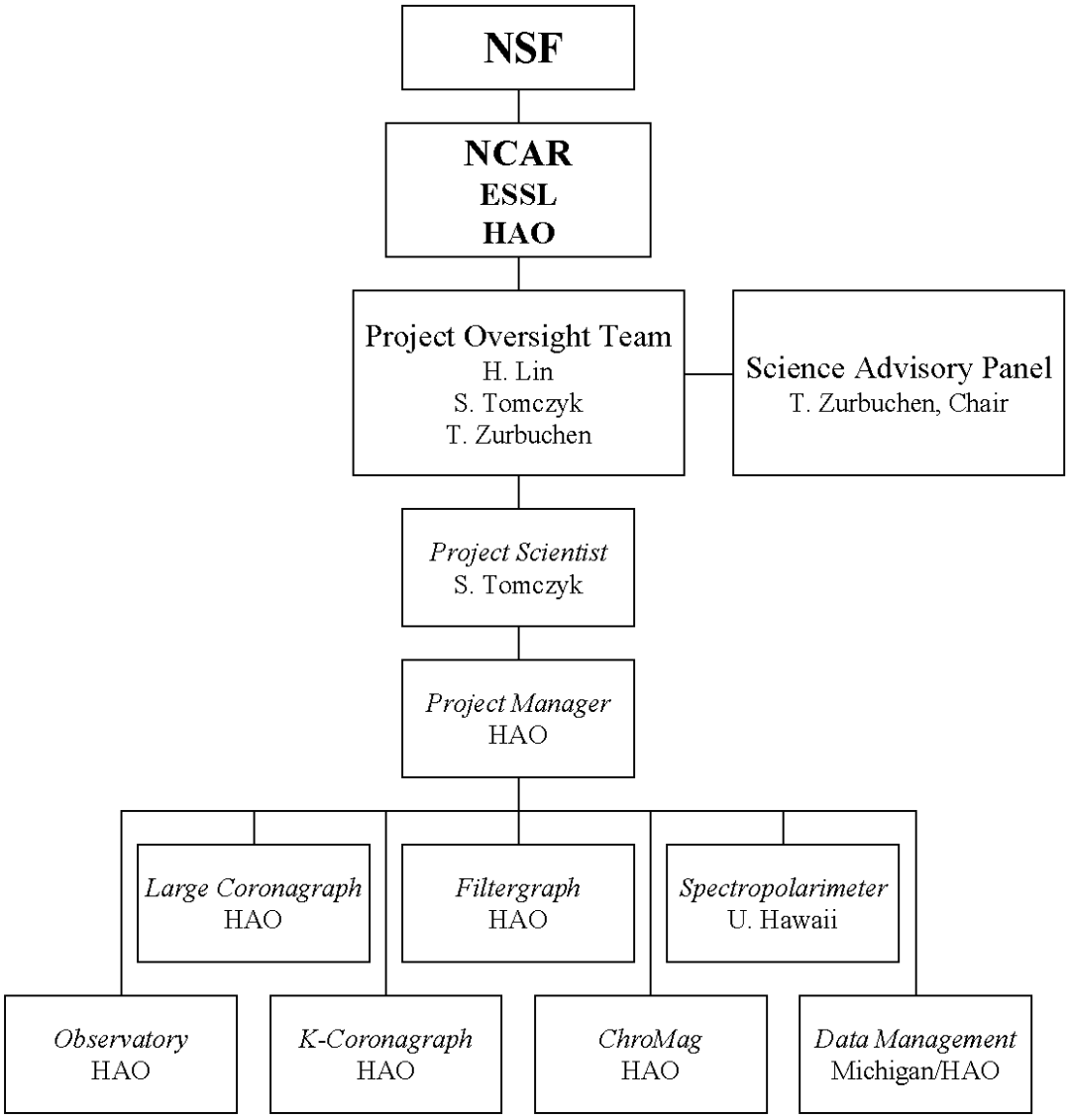

Figure 20 High-level organization chart

The Principal Investigators are supported by the COSMO Co-investigator team, which includes scientific, engineering, and administrative capacity to bring the project into operation:

- Joan Burkepile, Project Scientist III and MLSO Director of Operations, HAO/NCAR
- Roberto Casini, Scientist III, HAO/NCAR
- David Elmore, Research Engineer, HAO/NCAR
- Peter Fox, Computational Scientist, HAO/NCAR
- Phil Judge, Senior Scientist, HAO/NCAR

- Jeff Kuhn, Professor, University of Hawaii
- Boon Chye Low, Senior Scientist, HAO/NCAR
- Scott McIntosh, Project Scientist II, HAO/NCAR
- Peter Nelson, Engineer III, HAO/NCAR
- Stanley C. Solomon, Senior Scientist and Deputy Director, HAO/NCAR

7.1.3 Community Participation

A key element of the user community includes US universities pursuing solar and heliospheric research. According to the 2000-2010 National Research Council decadal review, there is a need for direct community involvement in solar observational methods and primary data analysis (Lanzerotti 2003). COSMO will address this need through collaborations that make the university community an integral part of the entire COSMO effort. The University of Michigan and the University of Hawaii are partners in the design and construction of the COSMO project. The SAP (and eventually the UAP, which will oversee continuing scientific operation) has leadership and key representatives from the university research community.

In addition, the organization of the COSMO project provides direct access for undergraduate, masters, and Ph.D. students and their advisors to breakthrough instrument development in modern solar physics. Community outreach programs at HAO/NCAR, such as the visiting faculty program and others already offer access to COSMO. New HAO/NCAR summer programs will offer opportunities for undergraduate and master's students. In addition, COSMO Ph.D. fellowships will focus on technology development and data analysis from this new observing facility to offer hands-on research experience.

International and US collaborators will be invited through community engagement and communication strategies. A Web site is being developed for the broad distribution of project information. Regular project status messages to internal and external stakeholders will be released by management of the project team. Teleconference and videoconference meetings ("town hall" sessions) will be conducted at periodic intervals with the SAP/UAP. For the widest distribution, presentations on the project will be made during scientific and/or engineering meetings.

7.1.4 Science Advisory Panel (SAP)

The COSMO management approach requires the scientific user community to direct the design, operation, and use of data from the new facility. The COSMO Science advisory Panel was formed in 2005 to advise the COSMO team. Members of the panel represent university, federal, private, and international institutions. By April 2007, the SAP has met once, conducted several teleconferences, and developed the scientific and research questions in the form of technical memos that directed the specifications and performance requirements of the instruments. They have also worked to guide the anticipated data products emanating from the COSMO data stream. The current membership of the SAP is:

- Thomas Zurbuchen, University of Michigan (Chair)
- David Alexander, Rice University
- Spiro Antiochos, Naval Research Laboratory
- Jean Arnaud, Université de Nice, France

- Phil Judge, High Altitude Observatory, NCAR
- Matt Penn, National Solar Observatory
- John Raymond, Harvard Smithsonian Center for Astrophysics
- Aad VanBallegooijen, Harvard Smithsonian Center for Astrophysics

Panel members will start to rotate off the panel on staggered three-year terms after commencement of the project. Replacements will be identified through nomination by directors of leading university departments and national laboratory divisions in the solar physics area, and they will be selected by vote of the existing panel.

7.1.5 User Advisory Panel (UAP)

Once the COSMO facility is operational, the SAP will transition to a User Advisory Panel, which will advise the COSMO team and will become a crucial link between user needs and the new facility. The UAP will include international as well as national representatives of the solar and heliospheric research community. Panel members will serve staggered three-year terms after commencement of operations. Replacements will be identified through nomination by directors of leading university departments and national laboratory divisions in the solar physics area. Selection will be by vote of the existing panel.

Observing campaigns and user observing programs will be conducted in a manner similar to the SOHO JOPs. The UAP will provide feedback on data products and data dissemination, give input on future instrument upgrades, and develop metrics for monitoring the quality of scientific return.

The COSMO facility will also provide easy access to test breakthrough technology development funded through independent investigations. The multi-instrument nature of the COSMO facility enables this interaction without jeopardizing the primary science. The COSMO UAP will oversee the selection of such instrument testing.

7.2 Management Methodology

7.2.1 Technical Project Management

Technical management of the COSMO project will be performed by a full-time project manager at HAO/NCAR (who will also participate in systems engineering activities) under the direction of Steven Tomczyk. Individual engineering leads will be identified for the four major instrument systems that are the responsibility of HAO/NCAR, and for the management of the observatory building contractor. The spectropolarimeter instrument is the responsibility of University of Hawaii, and will be managed under the direction of Haosheng Lin. Data system development will occur jointly at University of Michigan and HAO; the Michigan component will be managed under the direction of Thomas Zurbuchen. These aspects of the program will fall under the technical leadership of the HAO project manager, but will maintain their own budget and schedule tracking and have individual responsibility for delivery and quality assurance.

Standard project tracking and planning tools will be used to conduct technical management of the COSMO project. These will include:

- A project schedule tracking system (e.g., Microsoft Project) to provide detailed task-oriented status reporting, dependency network and critical path analysis, and summary overviews.

- An Earned Value Management System (EVMS) to provide diagnostic and forecasting information about the cost performance of the program, budget variance data including final cost projection, and trend analysis over the project lifecycle.

The COSMO project is characterized by several large-scale procurement items and sub-contracts, including the lens, telescope, detectors, building, and domes. Contracting, supervising, and tracking these efforts will be a critical concern of the project manager. Expertise from the UCAR contracting office, which has worked effectively with HAO engineering in the past and assisted considerably in the costing effort for this prospectus, will be of great value to the program. An important part of vendor management will be a rigorously documented acceptance testing program as subsystem elements arrive.

Quality assurance will be maintained by a system of internal engineering peer review, exchange of engineers from other subsystems and other programs, and documentation of anomaly resolution. A detailed Performance Assurance plan for the project will be developed early in Phase B.

The current state of the project as of April 2007 is equivalent to a Phase-A conceptual design and definition study. This is due to the success of the prototype detector developed at HAO/NCAR and at University of Hawaii and investment by the NCAR Initiative program in conceptual design and costing work for a large-aperture coronagraph and supporting instrumentation. We anticipate that the Phase-A study will be completed during the summer of 2007. An informal Conceptual Design Review (CoDR) will be held in fall 2007.

Three other major reviews are anticipated during the course of the project as outlined in Section 7.4. The most important of these is the Preliminary Design Review at the conclusion of Phase B, approximately one year into the design and development phase of the project.

Routine project reporting will occur through annual project reports and quarterly financial updates. In order to maintain communication, an informal monthly newsletter will be distributed to all project personnel, the SAP, institutional and foundation management, and other interested parties in the scientific community. Presentations, briefings, informal updates, and discussions will be held in conjunction with regular scientific meetings and workshops. A focused workshop for the user community will be held in conjunction with "first light," currently estimated to take place shortly after the Qualification Review at the end of the fourth year of the project.

7.2.2 Risk Management

The risk assessment, monitoring, and mitigation procedures described here allow the project team to respond to the dynamic risk environment surrounding the life of the COSMO design and development phase. We have assessed the initial key risk factors and have planned for how risks will be monitored and mitigated as the project proceeds. The initial risk assessment provides a baseline view of the project risk environment and an important sense of key factors that may have an influence on effective execution of the program. We will monitor risk over the

course of the project, review the defined risk areas at regular intervals, and retire and/or add new risks as needed. A baseline risk assessment will be supplemented by ongoing risk monitoring, assessment, and mitigation during COSMO design and construction and will continue on during its operational lifetime. Should any significant areas of concern be identified during the regular reviews, the HAO/NCAR team and the UAP will develop mitigation strategies.

There are three basic categories of risk: internal, external, and environmental. In the full COSMO proposal, we will include a detailed risk assessment that assesses specific risks within each category, assigns specific risk owners to monitor and address them, and discusses mitigation strategies. In this document, we identify and categorize significant risks that we anticipate may impact the project development schedule and budget.

Internal risks

Internal risks are those that are primarily owned by HAO/NCAR, University of Michigan, and University of Hawaii. Significant optics design work has been completed and will be described in more detail in the full COSMO proposal. This key element of the facility relies on interdependent elements that flow from the science goals and achievable technological performance. The time and labor needed for additional design work could exceed original estimates. Mitigation involves careful monitoring of this task and quick response with contingency funds if needed to keep the project on schedule for purchasing components. Specific examples of known internal risks are:

- Detailed optical design studies reveal performance issues with critical elements
- Design falls behind schedule due to lack of adequate personnel resources
- Vendor bids and subcontracting delayed due to administrative issues
- Fabrication exceeds cost estimates or time estimates
- Software development becomes excessively complex

External risks

External risks are those that, to a large degree, are not controlled by HAO/NCAR, University of Michigan, or University of Hawaii, but are owned by outside parties. In some cases, these outside parties are the regulatory bodies governing site selection, infrastructure, construction, and fabrication. In most others, these are essentially risks due to vendor issues. Mitigation will involve maintaining alternatives as long as possible, anticipating long lead times on crucial procurements, responding to trouble indicators, and conducting careful acceptance testing. Specific examples of known external risks are:

- Site permitting for facility encounters regulatory difficulties
- Building contractor fails to meet cost and/or schedule bid
- Lens polishing exceeds cost or time estimates, or fails to meet specifications
- Vendor issues with telescope, optics, or detectors
- Delivery or deployment issues cause problems with final performance

Environmental risks

Environmental risks are those that arise from acts of nature or from attitudes and perceptions about the COSMO project from the culture surrounding the program. This culture consists of the scientific stakeholders of the project, the project sponsors (NSF), and other parties. Assuming adequate technical performance, the risk of a dissatisfied user community is considered low, due to the extensive community-led definition effort. However, the natural environment on Hawaii is an obvious and considerable risk factor. Specific examples of known environmental risks are:

- Volcanic eruption
- Typhoon
- Degradation of divisional infrastructure

7.2.3 Operational Management

The MLSO facility staff will bring their expertise and current level of support from HAO/NCAR to the COSMO facility. When COSMO is complete, the existing MLSO observatory building and equipment will be decommissioned, making both the observing personnel in Hawaii and the data management personnel in Boulder available for COSMO operations. Only one data management FTE will be added to the Boulder operation, thereby limiting incremental recurring costs during the operational phase.

COSMO operations will be managed by Joan Burkepile of HAO/NCAR, who currently directs MLSO operations. She will be responsible for raw data relay and initial processing, archiving at the NCAR Data Center, and relaying to the Principal Investigator institutions. HAO/NCAR will also participate in development of science analysis products, quick-look products, and educational/outreach products. Operations will be conducted in response to oversight by the UAP, as described in Section 7.1.5.

Thomas Zurbuchen will lead the development of data analysis and model comparison software at the University of Michigan. During the operation phase, University of Michigan and University of Hawaii will participate in dissemination of analysis products and scientific exploitation of the results.

7.2.4 Data Distribution

All relevant synoptic and campaign data, as defined by the SAP, will be made available to the scientific community and the general public. To assure the appropriate sharing of credit, proper citation, and scientific interpretation, a basic “rules of the road” document will be prepared by the SAP, similar to the practice by the NSF CEDAR community.

The data dissemination process will follow strategies developed for the MLSO facility (see Section 4), which provides complete on-line Internet access to all data and archives. Mauna Loa data are used by hundreds of scientists and students from more than 150 institutions worldwide (see Section 9.2). We expect to serve scientists at these institutions and more with open access to COSMO data.

HAO/NCAR has operated and maintained the Mauna Loa Solar Observatory since 1965 with three full-time observers at Mauna Loa and three full-time staff at HAO/NCAR to process, calibrate, archive, and distribute all observations in near real time. HAO/NCAR will continue to provide this level of support to the COSMO observatory. Similar programs have also developed at University of Michigan for space flight instrumentation, and this experience is also available to the COSMO team through Principal Investigator Thomas Zurbuchen.

In addition to generating an enormous resource of synoptic data, the scientific impact of the COSMO facility will be expanded in future years through targeted observational campaigns. These will require coordination between the COSMO instruments and other observational tools on the ground or in space. The methodology for enhanced science impacts pioneered by the SOHO joint observation program will be used for COSMO.

7.3 Budget

7.3.1 Budget Methodology

We have performed a preliminary analysis of the anticipated cost of the COSMO facility through contractor bids, engineering analysis, and building planning. Highlights of the methodology for estimating the most significant items are summarized here:

- Cost of the lens blank and rough grinding were obtained from a sole-source price quote from Corning.
- Lens polishing bids were obtained from four vendors. The cost carried in the budget represents the mean of the four quotes.
- The telescope cost was obtained by taking the mean of two cost estimates from candidate vendors.
- Cost of relay optics was obtained by a single source quote.
- Narrow-band filter polarimeter cost estimates resulted from detailed analysis by HAO engineering personnel. The estimate for detectors was obtained by a sole-source quote from Teledyne, and an estimate for the Lyot filter was obtained from a single-source Meadowlark Optics quotation.
- Spectropolarimeter cost estimates were performed by University of Hawaii engineering personnel. The camera system cost was obtained by single-source Teledyne quotation.
- A solar-pointed spar will be provided free of charge through an agreement with the NSO. It will be employed if the Mauna Loa site is selected. If Haleakala is selected, the existing Mees observatory spar will be used.
- K-coronagraph cost estimates resulted from detailed analysis by HAO engineering personnel. The estimate for detectors was obtained from a sole-source Sarnoff quotation.
- ChroMag cost estimates resulted from detailed analysis by HAO engineering personnel. The estimate for detectors was obtained from a sole-source Teledyne quotation, and the estimate for the Lyot filter was obtained from a sole-source Meadowlark Optics quotation.

- The building estimate was obtained from detailed costing by UCAR facilities management director John Pereira. An elevator estimate was obtained from a single-source quotation. The 12.2-m dome estimate is the mean of two quotations by vendors; the 5-m dome estimate is the mean of a single-source quotation and an estimate of the costs to refurbish and ship a dome obtained free of charge from the NSO.
- The Infrastructure/Environmental Impact cost estimate was obtained from Russ Schnell, operations chief of NOAA's Mauna Loa Observatory site.
- The data system estimate was provided by detailed costing by University of Michigan for its portion of the project ($800K) and by HAO for the balance.
- Project management cost is estimated as $200K/year over five years, i.e., ~1 FTE. We anticipate that the project manager will be full time on the COSMO project, but will also participate in engineering tasks as time permits.

7.3.2 Budget Estimate

All engineering and support systems for the design and development effort are fully contained in the cost estimate. However, Scientist salaries at HAO/NCAR and the support of existing MLSO personnel are excluded from the budget, since they are covered by NSF base funding for this purpose.

All cost estimates have been performed with ample margins and conservative vendor and labor assumptions. A high-level summary of the budget estimate is shown in Table 4. The total project cost is estimated to be $22.6M.

7.3.3 Operations Budget Estimate

The recurring operational cost of the COSMO facility following conclusion of the design and development phase of the project will be borne mostly by the existing HAO operational effort. This consists of 3.0 FTE observing personnel at MLSO and 3.0 data management personnel at HAO in Boulder. Once COSMO is complete, regardless of its location, the existing MLSO facility will be closed and the HAO effort transferred to the new observatory. We do anticipate an increase in processing and reduction costs due to the much greater volume and complexity of the data. Therefore, we estimate that the annual incremental operational cost to NSF will be:

1 Data Management FTE $200K/year

In addition, we are requesting that NCAR increase the scientific staff at HAO by 1 FTE to develop an analysis and modeling effort commensurate with the scale of this new endeavor.

Item	Cost ($K)	Annual Breakdown ($K)				
		2009	2010	2011	2012	2013
Large Coronagraph						
Lens blank and grinding	662		662			
Lens polish	918			918		
Telescope	2,720				2720	
Relay optics	290				290	
Labor	423	127	84	106	106	
Subtotal	**5,013**					
Filtergraph						
Detectors	1,000			1000		
Lyot filters	500			500		
Hardware	505			160	345	
Labor	686	181	108	113	104	180
Subtotal	**2,691**					
Spectropolarimeter						
Camera system	1,100	1100				
Fiber-optic bundle	250	250				
Hardware	300	300				
Labor	829	114	258	251	110	96
Subtotal	**2,479**					
K-coronagraph						
Detectors	350			350		
Hardware	252			200	52	
Labor	1,048	212	142	146	151	397
Subtotal	**1,650**					
ChroMag						
Detectors	900			900		
Lyot filters	576			576		
Hardware	324				300	24
Labor	742	172	115	122	118	215
Subtotal	**2,542**					
Facility						
Infrastructure / env Impa	600		600			
Building	3,484		984	1600	900	
Elevator	134				134	
12.2-m dome	744				744	
5-m dome	23				23	
Subtotal	**4,985**					
Data System						
Labor	1,364	196	217	327	338	286
Computer equipment	170				60	110
Subtotal	**1,534**					
Project Management						
Subtotal	**1,168**	220	227	233	240	248
Travel and Shipping						
Subtotal	**573**	34	147	151	156	85
Total	**22,635**	**2,906**	**3,544**	**7,653**	**6,891**	**1,641**

Table 4 High-level summary of the budget estimate.

7.3.4 De-scope Plan

The COSMO project design and development will not exceed the proposed cost envelope. In order to assure that this is accomplished with minimum impact to the scientific goals, a detailed de-scope plan with cost saving estimates will be developed during the remainder of the Phase-A definition study. An outline of the major elements of this plan is given here.

Option 1—Reduce the aperture of the large-aperture coronagraph
The light-gathering requirements of the large-aperture coronagraph have been determined through the scientific requirements specified by the SAP and calculated through an error budget analysis (see Section 3.1.1). However, a modest reduction in size could be made, with the consequence of an increase in integration times and a loss of temporal resolution. This would reduce building costs as well as telescope costs. However, a decision to do this must be made early in Phase B because the lens and telescope acquisition sequence, as well as the building subcontract, must be started early.

Option 2—Eliminate the ChroMag and/or the K-coronagraph instruments
Eliminating the ChroMag and/or K-coronagraph would have serious impacts on the science capabilities of COSMO. Because the ChroMag development is phased to lag the other instruments, this option would remain viable as a late alternative.

7.4 Schedule

A high-level preliminary project schedule has been developed, showing that the COSMO design and development can be completed in five years, including a one-year Phase-B preliminary design study. The Phase-A definition study, now in progress at HAO/NCAR, will be completed during 2008. A Preliminary Design Review (PDR) will be held at the conclusion of Phase-B. A Critical Design Review (CDR) will be held approximately ten months later, and a Qualification Review will be held when the instrumentation systems are ready for final integration (see Figure 21).

The principal purpose of this preliminary plan is to determine the realism of cost phasing with regard to high-cost and long-lead-time instrument elements (e.g., the refractor) and subcontracts (e.g., the observatory building). One conclusion from this effort is that the large-aperture coronagraph lens blank will need to be purchased very early in the second year, prior to CDR. This is a significant investment, especially because it determines the ultimate telescope size. Therefore, the de-scope plan has been adjusted accordingly, to emphasize changes to supporting instrumentation and the detector system, rather than reducing the aperture dimension of the large-aperture coronagraph. This will be studied extensively during Phase B, but following PDR, this essential scale of the project will be determined. Therefore, PDR is the most important review in this sequence.

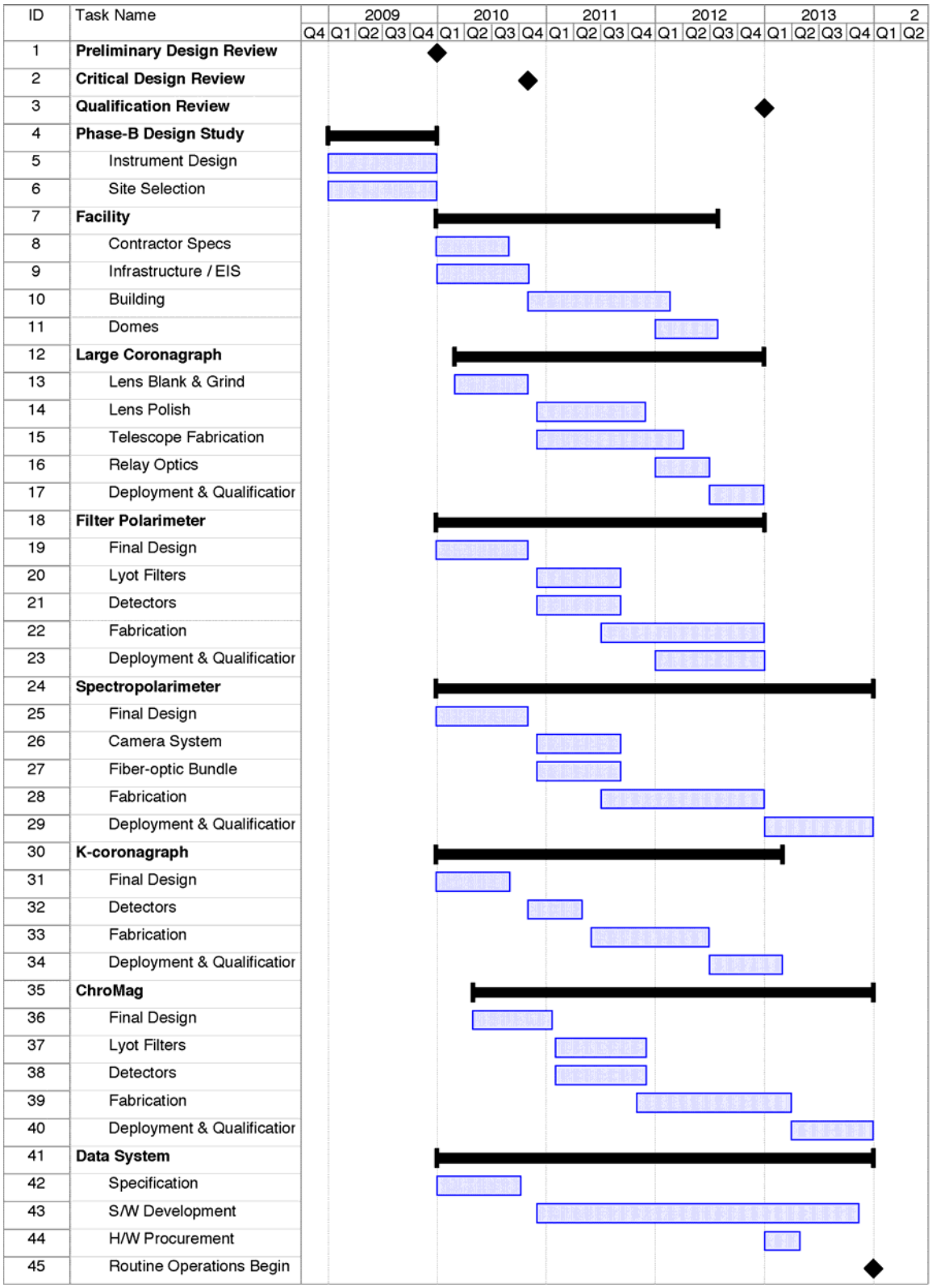

Figure 20 High-level project schedule

8 REFERENCES

Alexander, D., Metcalf, T. R. and Nitta, N. V. (2002). "Fast acceleration of a CME-related X-ray structure in the low solar corona." *Geo Res Letters*, **29**, 41.

Aschwanden, M. J., Fletcher, L., Sakao, T., Kosugi, T. and Hudson, H (1999). "Deconvolution of Directly Precipitating and Trap-precipitating Electrons in Solar Flare Hard X-Rays. III. Yohkoh Hard X-Ray Telescope Data Analysis." *Astrophysical Journal*, **517**, 977.

Bastian, T. S. (2004). "Low-frequency solar radiophysics with LOFAR and FASR." *Planetary and Space Science*, **52**, 1381.

Bommier, V., Landi Degl'Innocenti, E., Leroy, J.L., and Sahal-Brechot, S. (1994). "Complete determination of the magnetic field vector and of the electron density in 14 prominences from linear polarization measurements in the HeI D_3 and Hα lines." *Solar Physics*, **154**, 231.

Casini, R. (2007). "Prominence and Filament Magnetometry Simulations." *COSMO Tech Note 12*, Boulder, Colorado, High Altitude Observatory.

Casini, R. and Judge, P. G. (1999). "Spectral Lines for Polarization Measurements of the Coronal Magnetic Field. II. Consistent Treatment of the Stokes Vector for Magnetic-Dipole Transitions." *Astrophysical Journal*, **522**, 524.

Casini, R., López Ariste, A., Tomczyk, S. and Lites, B. W. (2003). "Magnetic Maps of Prominences from Full Stokes Analysis of the He I D3 Line." *Astrophysical Journal*, **598**, L67.

Charvin, P. (1965). "Etude de la polarisation de la raies interdites de la couronne solaire." *Annales d' Astrophisique*, **28**, 877.

Ciaravella, A., Raymond, J. C., Kahler, S. W., Vourlidas, A. and Li, J. (2005). "Detection and Diagnostics of a Coronal Shock Wave Driven by a Partial-Halo Coronal Mass Ejection on 2000 June 28." *Astrophysical Journal*, **621**, 1121.

Elmore, D. (2007a). "Baseline Design of a Coronagraph to Measure K-corona Polarization Brightness", *COSMO Tech Note 8*, Boulder, Colorado, High Altitude Observatory.

Elmore, D. (2007b). "Baseline Design for a Prominence Magnetometer", *COSMO Tech Note 11*, Boulder, Colorado, High Altitude Observatory.

Elmore, D. (2007c). "Mk4 Scattered Light Analysis." *COSMO Tech Note 10*, Boulder, Colorado, High Altitude Observatory.

Finsterle, W., Jefferies, S. M., Cacciani, A., Rapex, P. and McIntosh, S. W. (2004). "Helioseismic Mapping of the Magnetic Canopy in the Solar Chromosphere." *Astrophysical Journal*, **613**, L185.

Forbes, T. G. (2000), "A review on the genesis of coronal mass ejections." *Journal of Geophysical Research*, **105**, 23153.

Gosling, J. T. (1993). "The solar flare myth." *Journal of Geophysical Research*, **98**, 18937.

Gosling, J. T. and Hundhausen, A. J. (1995). "Reply (to Svestka 1995)." *Solar Physics*, **160**, 57.

Hanslmeier, A. (2003). "Space Weather - Effects on radiation on manned space missions." *Hvar Observatory Bulletin*, **27**, 159.

Harvey, J. W. (1969). "Magnetic Fields Associated with Solar Active-Region Prominences", University of Colorado, Boulder. **Ph.D. Thesis**.

Hayes, A. P., Vourlidas, A. and Howard, R. A. (2001). "Deriving the Electron Density of the Solar Corona from the Inversion of Total Brightness Measurements." *Astrophysical Journal*, **548**, 1081.

House, L. L. (1977). "Coronal emission-line polarization from the statistical equilibrium of magnetic sublevels. I - Fe XIII." *Astrophysical Journal*, **214**, 632.

Hundhausen, A. J. (1999). "Coronal Mass Ejections." *in The many faces of the Sun: a summary of the results from NASA's Solar Maximum Mission.* Edited by Keith T. Strong, Julia L. R. Saba, Bernhard M. Haisch, and Joan T. Schmelz. New York : Springer, 143.

Hyder, C. L. (1965). "The Polarization of Emission Lines in Astronomy. III. The Polarization of Coronal Emission Lines." *Astrophysical Journal*, **141**, 1382.

Iucci, N., Dorman, L. I., Levitin, A. E., Belov, A. V., Eroshenko, E. A., Ptitsyna, N.G., Villoresi, G., Chizhenkov, G. V., Gromova, L. I., Parisi, M., Tyasto, M. I. and Yanke, V. G. (2006). "Spacecraft operational anomalies and space weather impact hazards." *Advances in Space Research*, **37**, 184.

Jefferies, S. M., Osaki, Y., Shibahashi, H., Duvall, T. L., Jr., Harvey, J. W. and Pomerantz, M. A. (1994). "Use of acoustic wave travel-time measurements to probe the near-surface layers of the Sun." *Astrophysical Journal*, **434**, 795.

Jefferies, S. M., Osaki, Y., Shibahashi, H., Harvey, J. W., D'Silva, S. and Duvall, T. L., Jr. (1997). "Sounding the Sun's Chromosphere." *Astrophysical Journal*, **485**, L49.

Judge, P. G., Casini, R., Tomczyk, S., Edwards, D. P. and Francis, E. (2001). "Coronal Magnetometry: A Feasibility Study." *NCAR Technical Report* **NCAR/TN-446-STR**.

Judge, P. G. (2007). "Spectral lines for polarization measurements of the coronal magnetic field V: Information content of magnetic dipole lines." *Astrophysical Journal* **in press**.

Judge, P. G., Low, B. C. and Casini, R. (2006). "Spectral lines for polarization measurements of the coronal magnetic field. IV. Stokes signals in current-carrying field." *Astrophysical Journal*, **651**, 1229.

Kuhn, J. R., Coulter, R., Lin, H. and Mickey, D. L. (2003). "The SOLAR-C off-axis coronagraph." in Innovative Telescopes and Instrumentation for Solar Astrophysics, *Proc. SPIE*, **4853**, 318.

Lambour, R. L., Coster, A. J., Clouser, R., Thornton, L. E., Sharma, J., Cott, T. A. (2003). "Operational impacts of space weather." *Geophysical Research Letters*, **30**, 36.

Lanzerotti, L. J. (2003). "The Sun to the Earth - and Beyond, A Decadal Research Strategy in Solar and Space Physics." *N. R. C. Space Studies Board*, The National Academies Press, Washington, D.C.

Lanzerotti, L. J., Medford, L. V., Sayres, D. S., Maclennan, C. G., Lepping, R. P. and Szabo, A. (1998). "Space weather: Response of large-scale geopotentials to an interplanetary magnetic cloud." *Journal of Geophysical Research*, **103**, 9351.

Leroy, J. L. (1981). "Simultaneous measurement of the polarization in H-alpha and D3 prominence emissions." *Solar Physics*, **71**, 285.

Leroy, J. L., Bommier, V. and Sahal-Bréchot, S. (1984). "New data on the magnetic structure of quiescent prominences." *Astronomy & Astrophysics*, **131**, 33.

Lin, H., Kuhn, J. R. and Coulter, R. (2004). "Coronal Magnetic Field Measurements." *Astrophysical Journal*, **613**, L177.

Lin, H., Penn, M. and Tomczyk, S. (2000). "A New Precise Measurement of the Coronal Magnetic Field Strength." *Astrophysical Journal*, **541**, L83.

Longcope, D. W., Kankelborg, C. C., Nelson, J. L. and Pevtsov, A. A. (2001). "Evidence of Separator Reconnection in a Survey of X-ray Bright Points." *Astrophysical Journal*, **553**, 429.

Low, B. C. (1994). "Magnetohydrodynamic processes in the solar corona: Flares, coronal mass ejections and magnetic helicity." *Physics of Plasmas*, **1**, 1684.

Low, B. C. (2001). "Coronal mass ejections, magnetic flux ropes, and solar magnetism." *Journal of Geophysical Research*, **106**, 25141.

Low, B. C., Fong, B. and Fan, Y. (2003). "The mass of a solar quiescent prominence." *Astrophysical Journal*, **594**, 1060.

Low, B. C. and Zhang, M. (2002). "The Hydromagnetic Origin of the Two Dynamical Types of Solar Coronal Mass Ejections." *Astrophysical Journal*, **564**, L53.

Low, B. C. and Zhang, M. (2004). "Magnetostatic Structures of the Solar Corona. III. Normal and Inverse Quiescent Prominences." *Astrophysical Journal*, **609**, 1098.

McIntosh, S. W., Fleck, B. and Tarbell, T. D. (2004). "Chromospheric Oscillations in an Equatorial Coronal Hole." *Astrophysical Journal*, **609**, L95.

Nelson, P. G. (2006a). "An Analysis of Scattered Light in Reflecting and Refracting Primary Objectives for Coronagraphs." *COSMO Tech Note 4*. Boulder, CO, High Altitude Observatory.

Nelson, P. G. (2006b). "A FEA of Meter-Class Refracting Primary Objectives for Coronal Polarimetry." *COSMO Tech Note 2*, Boulder, Colorado, High Altitude Observatory.

Paletou, F., López Ariste, A., Bommier, V. and Semel, M. (2001). "Full-Stokes spectro-polarimetry of solar prominences." *Astronomy & Astrophysics*, **375**, L39.

Penn, M., Lin, H., Tomczyk, S., Elmore, D. and Judge, P. G. (2004). "Background-Induced Measurement Errors of the Coronal Intensity, Density, Velocity and Magnetic Field." *Solar Physics*, **222**, 61.

Perche, J. C. (1965). *CR Academy of Science*, **260**, 6036.

Querfeld, C. W. (1982). "The formation and interpretation of the Fe XIII 10747 Å coronal emission line." *Astrophysical Journal*, **255**, 764.

Querfeld, C. W., House, L. L., Smartt, R. N., Bommier, V., Landi Degl'Innocenti, E. (1985). "Vector Magnetic Fields in Prominences II - HeI D3 Stokes profiles analysis for two quiescent prominences." *Solar Physics*, **96**, 277.

Sahal-Bréchot, S. (1977). "Calculation of the polarization degree of the infrared lines of Fe XIII of the solar corona." *Astrophysical Journal*, **213**, 887.

Schmieder, B., van Driel-Gesztelyi, L., Aulanier, G.; Démoulin, P., Thompson, B.; de Forest, C., Wiik, J. E., Saint Cyr, C., Vial, J. C. (2002). "Relationships between CMEs and prominences." *Advances in Space Research*, **29**, 1451.

Sheeley, N. R., Jr, Howard, R. A., Koomen, M. J., Michels, D. J. (1983). "Associations between coronal mass ejections and soft X-ray events." *Astrophysical Journal*, **272**, 349.

Sime, D. G. and A. J. Hundhausen (1987). "The coronal mass ejection of July 6, 1980 - A candidate for interpretation as a coronal shock wave." *Journal of Geophysical Research*, **92**, 1049.

Svestka, Z. (1995). "On 'The Solar Flare Myth' postulated by Gosling." *Solar Physics*, **160**, 53.

Tomczyk, S. (2006a). "Measurement Errors in Coronal Magnetic Field Parameters." *COSMO Tech Note 1*. Boulder, High Altitude Observatory.

Tomczyk, S. (2006b). "Some Considerations for a High Etendue Birefringent Filter." *COSMO Tech Note 6*. Boulder, Colorado, High Altitude Observatory.

Tomczyk, S., McIntosh, S. W., Keil, S. L., Judge, P. G., Schad, T., Seeley, D. H. and Edmondson, J. (2007). "Alfvén waves in the Solar Corona." *Science*, **317**,1192.

Tomczyk, S., Card, G. L., Darnell, T., Elmore, D. F., Lull, R., Nelson, P. G., Streander, K. V., Burkepile, J., Casini, R., and Judge, P. (2008). "An Instrument to Measure Coronal Emission Line Polarization." *Solar Physics*, in press.

Trujillo Bueno, J., Landi Degl'Innocenti, E., Collados, M., Merenda, L. and Manso Sainz, R. (2002). "Selective absorption processes as the origin of puzzling spectral line polarization from the Sun." *Nature*, **415**, 403.

Van de Hulst, H. (1953). "The chromosphere and corona." *The Sun*. G. P. Kuiper**,** 207.

Vourlidas, A., Wu, S. T., Wang, A. H.;,Subramanian, P., Howard, R. A. (2003). "Direct Detection of a Coronal Mass Ejection-Associated Shock in Large Angle and Spectrometric Coronagraph Experiment White-Light Images." *Astrophysical Journal*, **598**, 1392.

Zhang, M., Dere, K. P., Howard, R. A., Kundu, M. R. and White, S. M. (2001). "On the temporal relationship between coronal mass ejections and flares." *Astrophysical Journal*, **559**, 452.

Zhang, M., Dere, K. P., Howard, R. A. and Vourlidas, A. (2004). "A study of the kinematic evolution of coronal mass ejections." *Astrophysical Journal*, **604**, 420.

Zolesi, B. and Cander, L. R. (2006). "Effects of the upper atmosphere on terrestrial and Earth space communications: Final results of the EU COST 271 Action." *Advances in Space Research*, **37**, 1223.

9 APPENDICES

9.1 Additional Material

These and other references are available at http://www.cosmo.ucar.edu.

9.1.1 Technical Notes

Technical notes are available at http://www.cosmo.ucar.edu/tech-notes.jsp.

Coronal Magnetometry: A Feasibility Study, P.G. Judge, R. Casini, S. Tomczyk, D.P. Edwards, E. Francis, January 2001.

Measurement Errors in Coronal Magnetic Field Parameters, S. Tomczyk, Tech Note 1, October 2006.

A FEA of Meter-Class Refracting Primary Objectives for Coronal Polarimetry, P. Nelson, Tech Note 2, October 2006.

Polarization in Reflecting and Refracting Coronagraphs, D. Elmore, Tech Note 3, October 2006.

An Analysis of Scattered Light in Reflecting and Refracting Primary Objectives for Coronagraphs, P. Nelson, Tech Note 4, October 2006.

Trade Study Summary for Reflecting vs. Refracting Primary Objectives for the COSMO Large Coronagraph, P. Nelson, D. Elmore and S. Tomczyk, Tech Note 5, November 2006.

Some Considerations for a High Etendue Birefringent Filter, S. Tomczyk, Tech Note 6, October 2006.

Scattered Light from Internal Reflection in a Coronagraph Objective Lens, S. Tomczyk, Tech Note 7, October 2006.

Baseline Design of a Coronagraph to Measure K-corona Polarization Brightness, D. Elmore, Tech Note 8, January 2007.

SBM Sky Brightness at Mauna Loa, D. Elmore, Tech Note 9, January 2007.

Mk4 Scattered Light Analysis, D. Elmore, Tech Note 10, January 2007.

Baseline Design of a Prominence and Filament Magnetometer, D. Elmore, Tech Note 11, January 2007.

Prominence and Filament Magnetometry Simulations, R. Casini, Tech Note 12, January 2007.

A Thermal Analysis of a 1.5 meter f/5 Fused Silica Primary Lens for Solar Telescopes, P. Nelson, Tech Note 13, February 2007.

9.1.2 Relevant Papers

Reprints and preprints are available at http://www.cosmo.ucar.edu/journal-articles.jsp.

Casini, R. and P. Judge (1999). "Spectral Lines for Polarization Measurements of the Coronal Magnetic Field. II. Consistent Treatment of the Stokes Vector for Magnetic-Dipole Transitions." *Astrophysical Journal*, **522**, 524.

Judge, P. G. (2007). "Spectral lines for polarization measurements of the coronal magnetic field V: Information content of magnetic dipole lines." *Astrophysical Journal* **in press**.

Judge, P.G. (1998). "Spectral lines for polarization measurements of the coronal field. I theoretical intensities." *Astrophysical Journal*, **500**, 1009.

Judge, P. G., B. C. Low and Casini, R. (2006). "Spectral lines for polarization measurements of the coronal magnetic field. IV. Stokes signals in current-carrying field." *Astrophysical Journal* **651**, 1229.

Lin, H., J. R. Kuhn and Coulter, R. (2004). "Coronal Magnetic Field Measurements." *Astrophysical Journal*, **613**, L177.

Lin, H., Penn, M. and Tomczyk, S. (2000). "A New Precise Measurement of the Coronal Magnetic Field Strength." *Astrophysical Journal*, **541**, L83.

Penn, M., Lin, H., Tomczyk, S., Elmore, D. and Judge, P.G. (2004). "Background-Induced Measurement Errors of the Coronal Intensity, Density, Velocity and Magnetic Field." *Solar Physics*, **222**, 61.

Tomczyk, S., McIntosh, S.W., Keil, S.L., Judge, P.G., Schad, T., Seeley, D.H., Edmondson, J., Observation of Alfvén waves in the Quiet Solar Corona, *Science*, **317**, 1192.

Tomczyk, S., Card, G. L., Darnell, T., Elmore, D. F., Lull, R., Nelson, P. G., Streander, K. V., Burkepile, J., Casini, R., and Judge, P. (2007). "An Instrument to Measure Coronal Emission Line Polarization." *Solar Physics*, in press, 2008.

9.2 User Community for Mauna Loa Data

A Partial List of Scientific Institutions Using Data (2001-2006) from the Mauna Loa Solar Observatory has been compiled. Users at these 142 Institutions requested coronal and solar images, information, and analysis in addition to data directly available from the Mauna Loa Solar Observatory (MLSO) Web site from 2001 to 2006. Many users of MLSO data only retrieve the observations directly from the MLSO Web site, and so their organizations may not be included here.

MLSO data are available at http://mlso.hao.ucar.edu.

9.2.1 National Users

Air Force Research Laboratory Headquarters, Phillips Lab, Hanscom AFB, MS

Air Force Weather Agency, Bellevue, NE
Alabama A & M University, Normal, AL
Arizona State University, Phoenix, AZ
Augsburg College, Minneapolis, MN
Boston College, Chestnut Hill, MA
Boston University, Boston, MA
California Institute of Technology, Pasadena, CA
California State, Northridge, CA
Catholic University of America, Washington, DC
Center for Astrophysics, Cambridge, MA
Denver Museum of Nature and Science, Denver, CO
E. O. Hulburt Center for Space Research, Naval Research Laboratory, Washington, DC
Exploration Physics International, Huntsville, AL
George Mason University, Fairfax, VA
Hanscom Air Force Base, MS
Harvard University, Cambridge, MA
Harvard-Smithsonian Center for Astrophysics, Cambridge University, Cambridge, MA
Helio Research, La Crescenta, CA
Helio Synoptics, Boulder, CO
Jet Propulsion Laboratory, Pasadena, CA
Johns Hopkins University, Laurel, MD
Joint Astronomy Centre, Hilo, HI
L-3 Com/GSI, Largo, MD
Lockheed Martin, Palo Alto, CA
Los Alamos National Laboratory, Los Alamos, NM
Maryland Science Center, Baltimore, MD
Massachusetts Institute of Technology, Cambridge, MA
Middlebury College, Middlebury, VT
Montana State University, Bozeman, MT
NASA Ames Research Center, Moffett Field, CA
NASA Goddard Space Flight Center, Greenbelt, MD
NASA Headquarters, Washington, DC
NASA Marshall Space Flight Center, Huntsville, AL
National Center for Atmospheric Research, RAP Division, Boulder, CO
National Geophysical Data Center, Boulder, CO
National Optical Astronomy Observatories, Tucson, AZ
National Radio Astronomy Observatory, Charlottesville, VA
National Solar Observatory, Sacramento Peak, NM
Naval Research Laboratory, Washington, DC
Oklahoma State University, Stillwater, OK
Oregon Episcopal Upper School, Portland, OR
Princeton University, Princeton, NJ
Rhodes College, Memphis, TN
Rice University, Houston, TX
SAIC, San Diego, CA
San Fernando Observatory, Sylmar, CA

Solar Consulting Services, New Smyrna Beach, FL
Solar Physics Research Corporation, Tucson, AZ
Southwest Research Institute, San Antonio, TX
Space Environment Center, NOAA, Boulder, CO
Stanford University, Palo Alto, CA
Texas Tech University, Lubbock, TX
University of Alabama, Huntsville, AL
University of California, Berkeley, CA
University of California, Los Angeles, CA
University of California, San Diego, CA
University of Colorado, Boulder, CO
University of Hawaii, Honolulu, HI
University of Illinois, Urbana, IL
University of Iowa, Iowa City, IA
University of Maryland, College Park, MD
University of Michigan, Ann Arbor, MI
University of New Hampshire, Durham, NH
University of North Carolina at Chapel Hill, Chapel Hill, NC

9.2.2 International Users

A.P.S. University, Rewa, India
ALROSA Co. Ltd, Moscow, Russia
Astronomical Institute of the Slovak Academy of Sciences, Tatranska Lomnica, The
Astronomical Observatory of Zagreb, Zagreb, Croatia, Slovak Republic
Beijing Astronomical Observatory, Beijing, China
British Broadcasting Corporation, London, United Kingdom
Calcutta University, Dept. of Applied Math, Calcutta, India
Chiba University, Chiba, Japan
Chinese Academy of Sciences, Space Science and Applied Research, Beijing, China
Communications Research Laboratory, Tokyo, Japan
Culgoora Solar Observatory, Narrabri, Australia
Dept. of Astronomy, Izmir, Turkey
Dominion Astrophysical Observatory, Saanich, Canada
Ege University Science Faculty, Izmir, Turkey
Freie Universität, Berlin, Germany
Hvar Observatory, Faculty of Geodesy, Zagreb, Croatia
Ibaraki University, Ibaraki, Japan
Imperial College, Lourdes, United Kingdom
Indian Institute of Astrophysics, Bangalore, India
Institut d'Astrophysique Spatiale, Orsay Cedex, France
Institut für Geophysik und Meteorologie, Universität zu Koln, Koln, Germany
Institut für HF-Technik, Universität Bochum, Bochum, Germany
Institute of Geophysics and Astronomy, Havana, Cuba
Institute of Solar-Terrestrial Physics, Irkutsk, Russia
Instituto de Astrofisica de Canarias, Tenerife, Spain

INAF Osservatorio Astronomico di Roma, Rome, Italy
ISAS, Kanagawa, Japan
IZMIRAN, Russian Academy of Sciences, Moscow, Russia
Karl-Franzens-Universität Graz, Graz, Austria
Kiepenheuer Institute, Freiburg, Germany
Kinki University, Osaka, Japan
Korea Astronomy and Space Science Institute, Daejeon, Korea
Korean Astronomy Observatory, Solar and Space Weather Group, Daejeon, Korea
Lund Observatory, Lund, Sweden
Max-Plank-Institut fur Aeronomie, Katlenburg-Lindau, Germany
Meisei University, National Astronomical Observatory of Japan, Tokyo, Japan
Mullard Space Science Laboratory, University College, London, UK
Nagoya University, Solar Terrestrial Environment Lab, Aichi, Japan
National Center for Radio Astrophysics, Maharashtra, India
National Central University, Taiwan, Japan
Nobeyama Radio Observatory, Nagano, Japan
Observatoire de Nice, Nice, France
Observatoire de Paris, Meudon, France
Osservatorio Astronomico di Capodimonte, Naples, Italy
Osservatorio Astronomico di Torino, Pino Torinese, Italy
Physical Research Lab, Atmospheric Science Division, Navrangpura, India
Physics Department, Zagreb, Croatia
Physikal Institute, Bern, Switzerland
Pulkovo Astronomical Observatory, St. Petersburg, Russia
Radioastronomisches Institut der Universität Bonn, Bonn, Germany
Radio Astronomy Lab, Natl. Commission on Aerospace Research & Development, Lima, Peru
Royal Observatory of Belgium, Brussels, Belgium
Rutherford Appleton Laboratory, United Kingdom
Solar Observatory, Kanzelhoehe, Austria
Solar Radio Laboratory, IZMIRAN, Troitsk, Russia
Sonnenobservatorium Kanzelhöhe, Treffen am Ossiacher See, Austria
Space and Atmospheric Physics Group, Blackett Laboratory, Imperial College, London, UK
Springbrook Research Observatory, Queensland, Australia
Udaipur Solar Observatory, Udaipur, India
Universidad de Loa Andes, Bogota, Colombia
University of Athens, Dept. of Physics, Athens, Greece
University of Birmingham, Birmingham, United Kingdom
University of Calgary, Calgary, Canada
University of Cambridge, Cambridge, United Kingdom
University of Florence, Florence, Italy
University of Glasgow, Glasgow, Scotland
University of Graz, Institute of Geophysics, Graz, Austria
University of Lethbridge, Lethbridge, Canada
University of Montreal, Dept. de Physique, Montreal, Canada
University of Rome, Rome, Italy
University of St. Andrews, St. Andrews, Scotland

University of Sydney, Sydney, Australia
University of Tokyo, Tokyo, Japan
University of Wales, Aberystwyth, United Kingdom
Upice Observatory, Upice, The Czech Republic

9.3 Glossary of Acronyms

ATST Advanced Technology Solar Telescope
CCMC Community Coordinated Modeling Center
CDR Critical Design Review
CHIP Chromospheric Helium-I Imaging Photometer
ChroMag Chromosphere and Prominence Magnetometer
CIS Cosmo Imaging Spectro-polarimeter
CME Coronal Mass Ejection
CoDR Conceptual Design Review
COMP Coronal Multi-channel Polarimeter
COPES Coordinated Observation and Prediction of the Earth System
COSMO Coronal Solar Magnetism Observatory
EIT Extreme ultraviolet Imaging Telescope
ESSL Earth and Sun Systems Laboratory (NCAR)
EUV Extreme Ultra Violet
FASR Frequency Agile Solar Radiotelescope
FEA Finite Element Analysis
FITS Flexible Image Transport System
FOV Field of View
FTE Full Time Equivalent
GOES Geostationary Operational Environmental Satellite
HAO High Altitude Observatory
IR Infra Red
JOP Joint Observing Program
LASCO Large Angle and Spectrometric Coronagraph
LOS Line Of Sight
LSST Large Synoptic Survey Telescope
MHD MagnetoHydroDynamics
MIST Modeled Integrated Scatter Tool
MLSO Mauna Loa Solar Observatory
NASA National Aeronautics and Space Administration
NCAR National Center for Atmospheric Research
NFP Narrowband Filter Polarimeter
NOAA National Oceanic and Atmospheric Administration
NSF National Science Foundation
NSO National Solar Observatory
NSWR National Space Weather Program
OFIS Optical Fiberbundle Imaging Spectropolarimeter
PB PetaByte
PDR Preliminary Design Review

PI Principal Investigator
PSF Point Spread Function
POS Plane Of Sky
PCA Principal Component Analysis
RMS Root Mean Square
SAP Science Advisory Panel
SDO Solar Dynamics Observatory
SECCHI Sun Earth Connection Coronal and Heliospheric Investigation
SEP Solar Energetic Particle
SHINE Solar Heliospheric and Interplanetary Environment
SOHO Solar and Heliospheric Observatory
SOLIS Synoptic Optical Long-term Investigations of the Sun
STEREO Solar TErrestrial RElations Observatory
TB TeraByte
TRACE Transition Region and Coronal Explorer
UAP User Advisory Panel
VSO Virtual Solar Observatory
VSTO Virtual Solar-Terrestrial Observatory

9.4 CVs of Key Personnel

Steven Tomczyk, Principal Investigator (PI)
Haosheng Lin, PI
Thomas Zurbuchen, PI

Steven Tomczyk

Biographical Sketch

Professional Preparation

Villanova University, B.S. Astronomy, 1979
University of California, Los Angeles, M.A. Astronomy, 1980
University of California, Los Angeles, Ph.D. Astronomy, 1988

Appointments

Visiting Scientist, 1988-90
High Altitude Observatory, National Center for Atmospheric Research
Scientist I, 1990–93
High Altitude Observatory, National Center for Atmospheric Research
Scientist II, 1993–97
High Altitude Observatory, National Center for Atmospheric Research
Scientist III, 1997–present
High Altitude Observatory, National Center for Atmospheric Research

Related Publications

Tomczyk, S., McIntosh, S.W., Keil, S.L., Judge, P.G., Schad, T., Seeley, D.H., Edmondson, J., Observation of Alfvén waves in the Quiet Solar Corona, *Science*, **317**, 1192.

Tomczyk, S., Card, G.L. Darnell, T., Elmore, D.F., Lull, R., Nelson, P.G., Streander, K.V., Burkepile, J., Casini, R., and Judge, P.G., An Instrument to Measure Coronal Emission Line Polarization, *Solar Physics*, in press, 2008.

Penn, M. J., Lin, H., Tomczyk, S., Elmore, D., Judge, P., Background-Induced Measurement Errors of the Coronal Intensity, Density, Velocity, and Magnetic Field, *Solar Physics*, **222**, 61, 2004.

Casini, R., López Ariste, A., Tomczyk, S., Lites, B. W., Magnetic Maps of Prominences from Full Stokes Analysis of the He I D3 Line, *ApJ*, **598**, L67-L70, 2003.

Judge, P.G., Tomczyk, S., Livingston, W.C., Keller, C.U., Penn, M.J., Spectroscopic Detection of the 3.934 Micron Line of Si IX in the Solar Corona, *ApJ*, **576**, L157-160, 2002.

Tomczyk, S., Streander, K.V., Card, G., Elmore, D., Hull, H., and Cacciani, A., An Instrument to Observe Low-Degree Solar Oscillations, *Solar Physics*, **159**, 1, 1995.

Selected Synergistic Activities

Co-investigator, SDO Helioseismic and Magnetic Imager Instrument
Member, NSO User's Committee
Member, ATST Coronal Working Group
Chair, HAO Instrumentation Advisory Committee

Haosheng Lin

Biographical Sketch

Professional Preparation

Tamkang University, Tamsui, Taiwan, B.S., Physics,1982
Michigan State University, Ph.D., Physics, 1992

Appointments

Assistant Engineer, Nov. 1984 - Aug. 1986
Electronics Research and Service Organization, Taiwan
Research Assistant, Jan. 1987 - Dec. 1992
Michigan State University
Research Associate, Jan. 1993 - Dec. 1994
California Institute of Technology
Research Scientist, Jan. 1995 - Dec. 1996
National Solar Observatory
Assistant Astronomer, Jan. 1997 - May 2000
National Solar Observatory
Assistant Astronomer, Jun. 2000 - June 2003
University of Hawaii
Associate Astronomer, July 2003 - present
University of Hawaii

Related Publications

Lin, H., and Versteegh, A., 2006, VisIRIS: a visible/IR imaging spectropolarimeter based on a birefringent fiber-optic image slicer, in Ground-based and Airborne Instrumentation for Astronomy, Proceeding of SPIE, 6269, 18, ed. McLean, I. S., and Masanori, I.., Orlando, Florida

Lin, H., 2004, Coronal Magnetic Field Measurements, ApJ, 613, L177

Lin, H., 2002, The Near-IR Spectropolarimeter of the advanced Technology Solar Telescope, in Innovative Telescopes and Instrumentation for Solar Astrophysics, Proceeding of SPIE, 4853, 215, ed. Keil, S. L., and Avakyan, S. V., Waiakoloa, Hawaii, 2002

Lin, H., Penn, M. J., and Tomczyk, S., 2000, New Precise Measurement of the Coronal Magnetic Fields, ApJ Letter, 541, 83L

Lin, H., and Casini, R., 2000, A Classical Theory of Coronal Emission Line Polarization, ApJ, 542, 528

Selected Synergistic Activities

Member, ATST Science Working Group
Member, ATST Site Survey Working Group
Lead Scientist, ATST Near-IR Spectropolarimeter
Principal Investigator, NSF/MRI Development of Instrumentation for High-Resolution and High-Precision Solar Magnetic Field Observations.
Principal Investigator, NSF Near-IR Study of Solar Magnetism project
Project Scientist, ATST Site Survey Sky Brightness Monitor project

Thomas H. Zurbuchen

Biographical Sketch

Professional Preparation

University of Bern, Masters in Physics, Astronomy and Mathematics, 1987-1992.
University of Bern, PhD in Astrophysics, 1992-1996.

Appointments

Research Fellow, University of Michigan, 1996–1998
Assistant Research Scientist, University of Michigan, 1998–2002
Senior research scientist, International Space Science Institute, Bern, Switzerland 2000–2001
Senior Associate Research Scientist, University of Michigan, 2002–2003
Associate Professor, University of Michigan, 2003–present

Related Publications

Zurbuchen, T. H., Connecting the Sun to the heliosphere, *EOS Transactions*, *88* (4), 37-42, 2007.

Zurbuchen, T. H., and D. F. Smart, Energetic particle acceleration and the injection problem: Who gets to play?, *Adv. Space Res.*, *37* (8), 1407, 2006.

Zurbuchen, T. H., and I. Richardson, In-situ solar wind and field signatures of interplanetary coronal mass ejections, *Space Sci. Rev.*, doi:10.1007/s11214-006-9010-4, 2006.

Zurbuchen, T. H., G. Gloeckler, F. Ipavich, J. Raines, C. W. Smith, and L. A. Fisk, On the fast coronal mass ejections in October/November 2003: ACE-SWICS results, *Geophys. Res. Lett.*, *31*, L11805, doi:10.1029/2004GL019461, 2004.

Zurbuchen, T. H., L. A. Fisk, G. Gloeckler, and R. Von Steiger, The solar wind composition throughout the solar cycle: A continuum of dynamic states, *Geophys. Res. Lett., 29* (9), 10.1029/2001GL013946, 2002.

Gloeckler, G., J. Geiss, N. A. Schwadron, L. A. Fisk, T. H. Zurbuchen, F. M. Ipavich, R. von Steiger, H. Balsiger, and B. Wilken, Interception of comet Hyakutake's ion tail at a distance of 500 million kilometers, *Nature*, *404*, 576, 2000.

Zurbuchen, T. H., S. Hefti, L. A. Fisk, G. Gloeckler, and N. A. Schwadron, Magnetic structure of the slow solar wind: Constraints from composition data, *J. Geophys. Res.*, *105*, 18,327, 2000.

Selected Synergistic Activities

2001-present Member, NASA Management Working Group for Solar and Heliospheric Physics
2002-present Member, ESA-NASA Solar Orbiter Instrument Definition Team
2004-present Member, NASA Science Definition Team for the Solar Sentinels Mission.
2004-2007 Deputy Chair, COSPAR Commission D on Space Plasmas in the Solar System
2004-present Member, National Academy of Sciences Committee on Solar and Space Physics
2005-present Member, NASA SPD Exploratory Committee
2006-present Member, Community Coordinated Modeling Center Science Working Group
2001-present Member, UM representative of the Space Science Working Group of the AAU
2003-present Member, AOSS Graduate Curriculum Committee
2006-2007 Member, UM Academic Affairs Advisory Committee